2020

Whitepaper: Understanding land-atmosphere interactions through tower-based flux and continuous atmospheric boundary layer measurements

Manuel Helbig

Tobias Gerken
gerkentx@jmu.edu

E Beamesderfer

D D. Baldocchi

T Banerjee

See next page for additional authors

Follow this and additional works at: https://commons.lib.jmu.edu/letfspubs

Part of the Atmospheric Sciences Commons, Climate Commons, and the Environmental Sciences Commons

Recommended Citation

Authors

Manuel Helbig, Tobias Gerken, E Beamesderfer, D D. Baldocchi, T Banerjee, S C. Biraud, N A. Brunsell, S P. Butterworth, W S. Chan, A R. Desai, J D. Fuentes, D Y. Hollinger, N Klijun, M Mauder, K A. Novick, J M. Perkins, C Rey-Sanchez, R L. Scott, B Seyednasrollah, P C. Stoy, R C. Sullivan, J Vilà-Guerau de Arellano, S Wharton, C Yi, and A D. Richardson

Understanding land-atmosphere interactions through tower-based flux and continuous atmospheric boundary layer measurements

Manuel Helbig[1,2], Tobias Gerken[3,4], Eric Beamesderfer[5], Dennis D Baldocchi[6], Tirtha Banerjee[7], Sebastien C. Biraud[8], Nathaniel A. Brunsell[9], Sean P. Burns[10,11], Brian Butterworth[12], W. Stephen Chan[8], Ankur R. Desai[12], Jose D. Fuentes[3], David Y. Hollinger[13], Natascha Kljun[14], Matthias Mauder[15], Kimberley A. Novick[16], John M. Perkins[17], Camilo Rey-Sanchez[6], Russel L. Scott[18], Bijan Seyednasrollah[5], Paul C Stoy[19], Ryan C. Sullivan[20], Jordi Vilà-Guerau de Arellano[21], Sonia Wharton[22], Chuixiang Yi[23], Andrew D. Richardson[5]

[1]School of Earth, Environment & Society, McMaster University

[2]Department of Physics and Atmospheric Science, Dalhousie University

[3]Department of Meteorology and Atmospheric Science, The Pennsylvania State University

[4]School of Integrated Sciences, James Madison University

[5]School of Informatics, Computing & Cyber Systems, Northern Arizona University

[6]Department of Environmental Science, Policy, and Management, University of California-Berkeley

[7]Department of Civil and Environmental Engineering, University of California-Irvine

[8]Earth and Environmental Sciences Area, Lawrence Berkeley National Laboratory, Berkeley, California

[9]Department of Geography and Atmospheric Science, University of Kansas

[10]Department of Geography, University of Colorado, Boulder, USA

[11]National Center for Atmospheric Research, Boulder, Colorado, USA

[12]Department of Atmospheric and Oceanic Sciences, University of Wisconsin-Madison

[13]USDA Forest Service, Northern Research Station, Durham, NC, USA

[14]Centre for Environmental and Climate Research, Lund University, Sweden

[15]Institute of Meteorology and Climate Research, Atmospheric Environmental Research (IMK-IFU), Karlsruhe Institute of Technology, Garmisch-Partenkirchen, Germany

[16]O'Neill School of Public and Environmental Affairs, Indiana University – Bloomington, USA

[17]Department of Hydrology and Atmosphere Sciences, University of Arizona, Tucson AZ

[18]Southwest Watershed Research Center, USDA-Agricultural Research Service

[19]Department of Biological Systems Engineering, University of Wisconsin-Madison

[20]Environmental Science Division, Argonne National Laboratory

[21]Meteorology and Air Quality Section, Wageningen University, Wageningen, The Netherlands

[22]Atmospheric, Earth and Energy Division, Lawrence Livermore National Laboratory, Livermore, California

[23]School of Earth and Environmental Sciences, Queens College, City University of New York

Executive summary

- ***Target audience:*** AmeriFlux community, AmeriFlux Science Steering Committee & Department of Energy (DOE) program managers [ARM/ASR (atmosphere), TES (surface), and SBR (subsurface)]

- ***Problem statement:*** The atmospheric boundary layer mediates the exchange of energy and matter between the land surface and the free troposphere integrating a range of physical, chemical, and biological processes. However, continuous atmospheric boundary layer observations at AmeriFlux sites are still scarce. How can adding measurements of the atmospheric boundary layer enhance the scientific value of the AmeriFlux network?

- ***Research opportunities:*** We highlight four key opportunities to integrate tower-based flux measurements with continuous, long-term atmospheric boundary layer measurements: (1) *to interpret surface flux and atmospheric boundary layer exchange dynamics at flux tower sites,* (2) *to support regional-scale modeling and upscaling of surface fluxes to continental scales,* (3) *to validate land-atmosphere coupling in Earth system models,* and (4) *to support flux footprint modelling, the interpretation of surface fluxes in heterogeneous terrain, and quality control of eddy covariance flux measurements.*

- ***Recommended actions:*** Adding a suite of atmospheric boundary layer measurements to eddy covariance flux tower sites would allow the Earth science community to address new emerging research questions, to better interpret ongoing flux tower measurements, and would present novel opportunities for collaboration between AmeriFlux scientists and atmospheric and remote sensing scientists. We therefore recommend that (1) a set of instrumentation for continuous atmospheric boundary layer observations be added to a subset of AmeriFlux sites spanning a range of ecosystem types and climate zones, that (2) funding agencies (e.g., Department of Energy, NASA) solicit research on land-atmosphere processes where the benefits of fully integrated atmospheric boundary layer observations can add value to key scientific questions, and that (3) the AmeriFlux Management Project acquires loaner instrumentation for atmospheric boundary layer observations for use in experiments and short-term duration campaigns.

1. Problem statement

The key question this white paper addresses is, "*How can adding atmospheric boundary layer measurements augment the scientific value of the AmeriFlux network?*" Specifically,

(1) what are the benefits, in the context of research on land-atmosphere interactions, of co-locating observations of aerodynamic and thermodynamic boundary layer properties (using balloon soundings, ceilometers, Doppler sodar, and radar wind profiles) with flux towers?

(2) What are the new science questions that could be investigated with these measurements? And,

(3) how would these measurements increase the long-term value of the AmeriFlux network, i.e., improve our understanding of coupled land-atmospheric feedback processes?

2. Background

Improving our understanding of land-atmosphere interactions is one of the key missions of the AmeriFlux network. Over the past few decades, eddy covariance based flux observations from the AmeriFlux network have been used to explore ecosystem responses to changes in atmospheric conditions (e.g., carbon dioxide concentrations, air temperature and humidity, drought) while relatively few studies have directly addressed feedback mechanisms between ecosystem and atmospheric processes. However, such feedback mechanisms (e.g., Raupach, 1998) likely exert important controls on the state of the biosphere [e.g., carbon storage (e.g., Green et al., 2019), soil moisture availability (e.g., Vogel et al., 2017), water balance (e.g., McNaughton & Spriggs, 1986; Salvucci & Gentine, 2013), and surface energy balance (e.g., Lansu et al., 2020)], cloud formation and patterns (e.g., Siqueira et al., 2009; Vilà-Guerau de Arellano et al., 2012), atmospheric chemistry and air pollution (e.g., Janssen et al., 2013), and future climate change trajectories (e.g., Davy & Esau, 2016). Additionally, the state of the lower atmosphere contains information that can help better constraining land surface processes and states [e.g., plant photosynthesis and respiration (Denning et al., 1999), soil water availability (Salvucci & Gentine, 2013)]. The interactions between land surface and atmosphere are mostly constrained to the atmospheric boundary layer (ABL, e.g., Yi et al., 2004), commonly defined as the lowest layer of the atmosphere (depth varies from a few meters to 1-3 km), which is directly influenced by land surface processes. The ABL links properties of soils, vegetation, and urban landscapes to the free troposphere and is of critical importance for weather, climate, and pollutant dispersion and chemistry. However, continuous ABL observations are rarely implemented across

the AmeriFlux network where the advantages of having co-located surface flux, radiation, and humidity measurements are numerous.

During daytime, the ABL is bounded by the land surface at its lower boundary and frequently by a capping thermal inversion at its upper boundary. The capping inversion is located where the vertical gradient of virtual potential air temperature and specific humidity changes rapidly with altitude, separating the ABL from the free troposphere (Fig. 1). The state of the ABL (e.g., air temperature and humidity, turbulence characteristics) is controlled by the exchange of heat, momentum, and scalars (e.g., water vapor, carbon dioxide, methane, aerosols) between land surface and ABL and between the free troposphere and ABL (Fig. 2). Diurnal growth of the convective ABL (CBL or mixed layer) causes warmer and typically drier air to be entrained into the ABL from the free troposphere. At the surface, the land-atmosphere exchange of heat, momentum, and scalars is mediated by the state of the ABL (e.g., evapotranspiration and carbon uptake response to atmospheric humidity and precipitation) and of the land surface (e.g., vegetation type, structure, phenology, and soil moisture).

The growth rate of the daytime ABL (or mixed layer) is mostly driven by thermal eddies, and thus depends on partitioning of the available energy at the land surface and specifically the split between latent and sensible heat fluxes, i.e. the Bowen ratio. If a greater portion of available energy is converted into sensible heat then this leads to a higher Bowen ratio, and the ABL grows more rapidly, while the opposite is true for a low Bowen ratio (i.e., ABL remains shallower when more energy input is latent heat). The rate of growth of the mixed layer is also determined by the strength of the capping inversion and subsequent entrainment (Driedonks & Tennekes, 1984; Wyngaard & Brost, 1984), the vertical rate of change of temperature and moisture, and the shear-mixing by wind (Batchvarova & Gryning, 1991).

At sunset, when solar heating of the surface ceases, buoyancy-driven turbulent mixing rapidly declines and the onset of the stable nocturnal ABL (NBL) occurs at the surface, leaving a residual layer aloft. The decoupling has important implications for the accuracy and interpretation of surface flux measurements, which require sufficient intensity of turbulent mixing to derive reliable eddy covariance fluxes. The NBL is characterized by a strong, shallow temperature inversion caused by surface radiative cooling. In contrast, potential air temperature and moisture in the residual layer is initially well-mixed but turbulence is weak and intermittent. A mechanistic understanding of the tight coupling between surface fluxes as measured by the eddy covariance technique (or other techniques such as scintillometry and flux gradients) and growth and decline of the ABL is thus essential to improve the current understanding of the land-atmosphere system and to properly account for dynamic atmospheric processes in studies of land-atmosphere interactions.
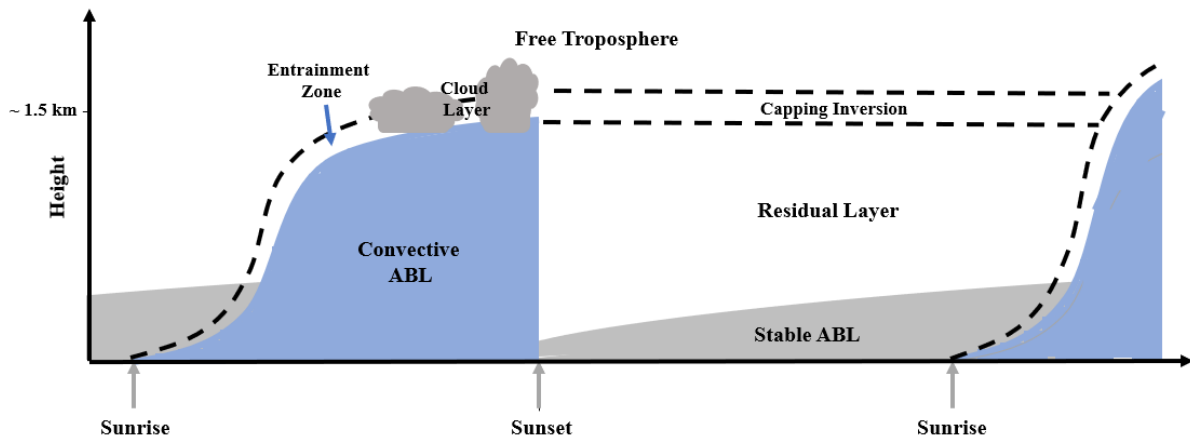
Fig. 1: Ideal diurnal development of the atmospheric boundary layer (ABL) during the day, from sunrise to sunset, and transformation to the stable ABL during the night from sunset to sunrise (figure after Stull, 1988).
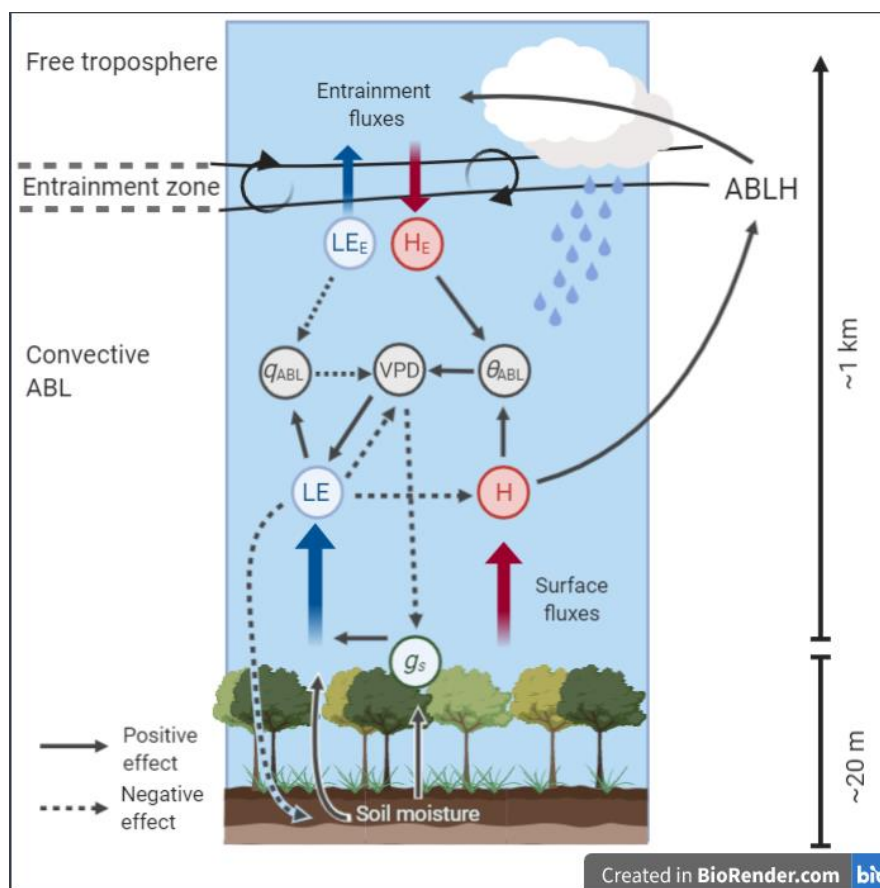
Fig. 2: Daytime feedbacks between surface energy fluxes (i.e., sensible heat flux [H], latent heat flux [LE]), entrainment fluxes (H_E, LE_E), land surface (e.g., soil moisture) and vegetation conditions (e.g., stomatal conductance [g_s]) and state of the atmospheric boundary layer (vapor pressure deficit [VPD], mixed-layer air temperature [θ_{ABL}], mixed-layer specific humidity [q_{ABL}]). The atmospheric boundary layer height (ABLH) separates the convective ABL from the free troposphere. Note that ABLH is not constant in time and that horizontal advection (not shown) will also impact ABL quantities. Figure was created with BioRender.com.

The ABL mixing height (ABLH) represents the thickness of the daytime ABL and is thus an indicator of the volume of air throughout which heat, momentum, and scalars may thoroughly mix. Surface emissions of aerosols, water vapor, and trace gases are uniformly mixed between surface and ABLH by convective and mechanical turbulence on a time scale from one to a few hours (e.g., Seibert et al., 2000; Yi et al., 2000; Yi et al., 2001).

The ABLH determines the height above ground to which air can be mixed and is a critical variable for understanding and constraining ecosystem and climate dynamics. For example, air pollutants in deep ABLs are well mixed, leading to lower pollutant concentrations (e.g., Yin et al., 2019). However, the dilution effect on ABL atmospheric carbon dioxide concentrations is not only due to mixing into a deep ABL but also due to the concurrent photosynthetic uptake of carbon dioxide (Yi et al., 2004) and due to the entrainment of air with lower carbon dioxide concentration at the top of the ABL (Vila-Guerau de Arellano et al., 2004). Given that ABLH controls the volume that is subject to mixing, Free troposphere-ABL differences in carbon dioxide concentrations covary with ABL depth on diurnal and seasonal timescales - also known as rectifier effect (e.g., Denning et al., 1995). This effect has direct implications for atmospheric carbon transport and its representation in atmospheric transport models (Denning et al., 1999).

The height of the ABL directly affects its heat capacity and therefore its potential to slow or enhance daily atmospheric warming rates (e.g., Panwar et al., 2019). ABL heights also play a crucial role for the onset of precipitation events and cloud dynamics (e.g., Juang et al., 2007; Konings et al., 2010; Siqueira et al., 2009). Convective clouds and locally generated precipitation only develop once the top of the ABL reaches the lifting condensation level (LCL, defined by the height where a parcel of moist air - lifted dry adiabatically from the surface - reaches saturation). The transition from clear to cloudy boundary layers has important implications for ABL dynamics. Cloud-ABL feedbacks lead to a reduction in ABL growth rate and drying of the subcloud layer, which is caused by enhanced entrainment and by moisture transport to the cloud layer (van Stratum et al., 2014). Convective cloud and precipitation development and deep convection will lead to deviations from the ABL behavior described above. For example, gust fronts associated with convective downdrafts quickly alter ABL state and consequently affect surface fluxes (e.g., Grant & Heever, 2016). Transitions from daytime to nighttime ABLs and from clear-sky to cloudy conditions also remain areas of current research.

Traditionally, ABLH has been derived from atmospheric profiles of air temperature and humidity measured by upper air sounding systems (e.g., balloon soundings). Such profile measurements are labor-intensive and are thus often made only a couple of times per day or are limited to short-term intensive field campaigns (Salcido et al., 2020). National weather service soundings are synchronized to noon and midnight UTC, not local time, so sample different parts of daily ABL

development (Fig. 1) depending on time zone. Recent progress in atmospheric observation techniques, specifically radar profilers and lidar-based devices, now allow us to continuously measure ABLH, automatically and at high temporal resolution. Instruments capable of such measurements are commercially available, relatively affordable (price similar to basic flux measurement instrumentation or high-precision laser-based gas analyzers), require minimal maintenance, and are suited to deployment even at remote field sites such as those typical of the AmeriFlux network. However, at present, direct ABL measurements are only made at a small fraction of sites across the AmeriFlux network (e.g., US-SGP, US-A03, US-A10, US-Ho1, US-KFS, US-Wkg, US-Wbw, and US-Tw1, US-Tw3) and, with some exceptions (e.g., US-KFS), ABL data are typically not submitted to the AmeriFlux network. In this white paper, we explore how extending co-located ABL observations (e.g., balloon soundings, ceilometers, radar profilers) across the AmeriFlux network could open new research opportunities and improve our mechanistic understanding of land-atmosphere interactions and feedbacks.

Tab. 1: List of definitions

| Term	Definition
Adiabatic process	Process during which an air parcel neither gains nor loses heat (e.g., latent heat of condensation).
Atmospheric boundary layer [ABL] (or planetary boundary layer)	Lower layer of the troposphere, which is directly influenced by the planetary surface. Roughly a few hundred meters to 1-2 km.
Atmospheric boundary layer height (or mixing height)	Thickness of the atmospheric boundary layer often characterized by a temperature inversion at the of the ABL. During daytime, the ABL height typically responds to surface forcing within a time scale of an hour to a few hours. In some cases, ABL growth may be capped by atmospheric subsidence. Mixing height refers to the height up to which heat, matter, and momentum originating from the land surface are well mixed through turbulent vertical mixing.
Capping inversion	Elevated inversion layer (i.e., reversal of temperature gradient) at the top of the ABL separating ABL from free troposphere
Convective boundary layer (or daytime boundary layer, mixed layer)	Type of ABL that is characterized by vigorous turbulence and mixing due to heating at the bottom of the ABL and entrainment at the top of the ABL during the day.
Entrainment	Process by which the turbulent mixed layer incorporates less turbulent air from the free troposphere leading to deepening of the mixed layer. Entrainment zone shear enhances entrainment and can contribute to rapid ABL growth. Typically, entrainment is associated with warming and drying of the ABL.
Free troposphere	Atmospheric layer above the ABL where the influence of the planetary surface (surface friction/drag) is minimal. Air in the free troposphere is warmer (for potential air temperature) and drier than in the ABL
Lifting condensation level	Level at which a parcel of moist air becomes saturated when lifted dry adiabatically
Nocturnal boundary layer	Cool stable layer adjacent to the ground developing during the night due to radiative cooling of the land surface. Mixing in the nocturnal boundary layer is mainly driven by shear-mixing (i.e., mechanical turbulence) and intermittent turbulence events.
Roughness sublayer	Lowest ABL adjacent to land surface and influenced by roughness elements (e.g., trees, buildings, vegetation). Layer depth is app. 2-5 times the height of roughness elements.
Surface layer	Bottom 10% of the ABL where mechanical generation of turbulence dominates

3. Overview of currently available technology

Various ground-based technologies are available for observations of aerodynamic and thermodynamic ABL properties (Table 2, e.g., Emeis et al., 2004; Wilczak et al., 1996). Here, we outline basic measurement principles of (1) balloon soundings, (2) ceilometers, (3) Doppler sodar, and (4) wind profiling radars and lidars.

Balloon soundings have been widely used for decades to detect ABL heights (e.g., Barr & Betts, 1997; Yi et al., 2001; Wang & Wang, 2014; Wouters et al., 2019, Salcido et al., 2020; most commonly used software to determine ABLH: Universal RAwinsonde OBservation program [raob.com]). Atmospheric profiles from balloon soundings provide detailed information on the vertical distribution of air temperature and humidity, air pressure, and wind speed and direction. The upper boundary of the ABL can be defined as the height where the maximum (i.e., positive) vertical gradient in potential temperature is located or as the height where the minimum (i.e., negative) vertical gradient of specific humidity is observed (coinciding with a sharp drop in specific humidity; Wang & Wang, 2014, Fig. 3). The vertical resolution of balloon soundings is usually lower than the vertical resolution of ceilometers (<30 m), and varies with atmospheric conditions and balloon ascent speed. Furthermore, balloons may travel tens of kilometers or more depending on advection such that the location of the derived ABL height is no longer within the footprint of the launch location. Wind speed and direction in the first few hundred meters are difficult to measure given the erratic motions of the sondes after launch. For this reason, sodars or lidars are well-suited instruments to co-locate with radiosondes. Balloon soundings represent the most labor-intensive way of measuring ABL height requiring ongoing costs for manual labor. Global networks of synoptic observation sites provide daily balloon sounding data, which are archived in the Integrated Global Radiosonde Archive (Durre et al., 2006; available through the NOAA National Centers for Environmental Information) and in the University of Wyoming sounding data archive (http://weather.uwyo.edu/upperair/sounding.html). However, measurements are typically only conducted twice a day (at 00 and 12 UTC) and lack information about the diel cycles of ABL development. Also, the launch points are fixed and may not represent the air masses surrounding AmeriFlux sites.

Ceilometers emit a laser pulse (wavelength between 300 and 1500 nm), which is scattered in the atmosphere by aerosols. A portion of this scatter is directed back to the receiver and recorded as backscatter. Thus, ceilometers produce aerosol profiles for each laser pulse, which can be used to derive cloud ceiling and ABL height (Kotthaus & Grimmond, 2018a). The ABL depth in this case is typically defined as the height at which aerosol concentration and thus the backscatter signal decreases sharply (Fig. 4). Therefore, the ability of a ceilometer to detect ABL depths depends on the level of aerosol concentrations in the ABL and on the sensitivity of the instrument to small aerosol particles. In clean air, retrievals of ABL

heights may therefore be problematic. The advantage of the ceilometer is that it allows continuous observations of ABL height and that it is a relatively inexpensive instrument. Additionally, ceilometers provide information on the location of cloud base and cover. In contrast to balloon soundings, ceilometers do not measure atmospheric profiles of temperature and humidity and thus do not allow the derivation of potential temperature and specific humidity gradients in the free troposphere. However, these gradients are essential for the calculation of entrainment fluxes (van Heerwaarden et al., 2009). To add information on atmospheric humidity profiles, ceilometers can be paired with water vapor lidar instruments (e.g., compact water vapor differential absorption lidar), which allow continuous measurements of water vapor profiles up to a few kilometers above ground. Alternatively, combining ceilometers with balloon soundings can provide such information. Paired observation systems can therefore give new insights into complex feedback mechanisms between land and atmosphere.
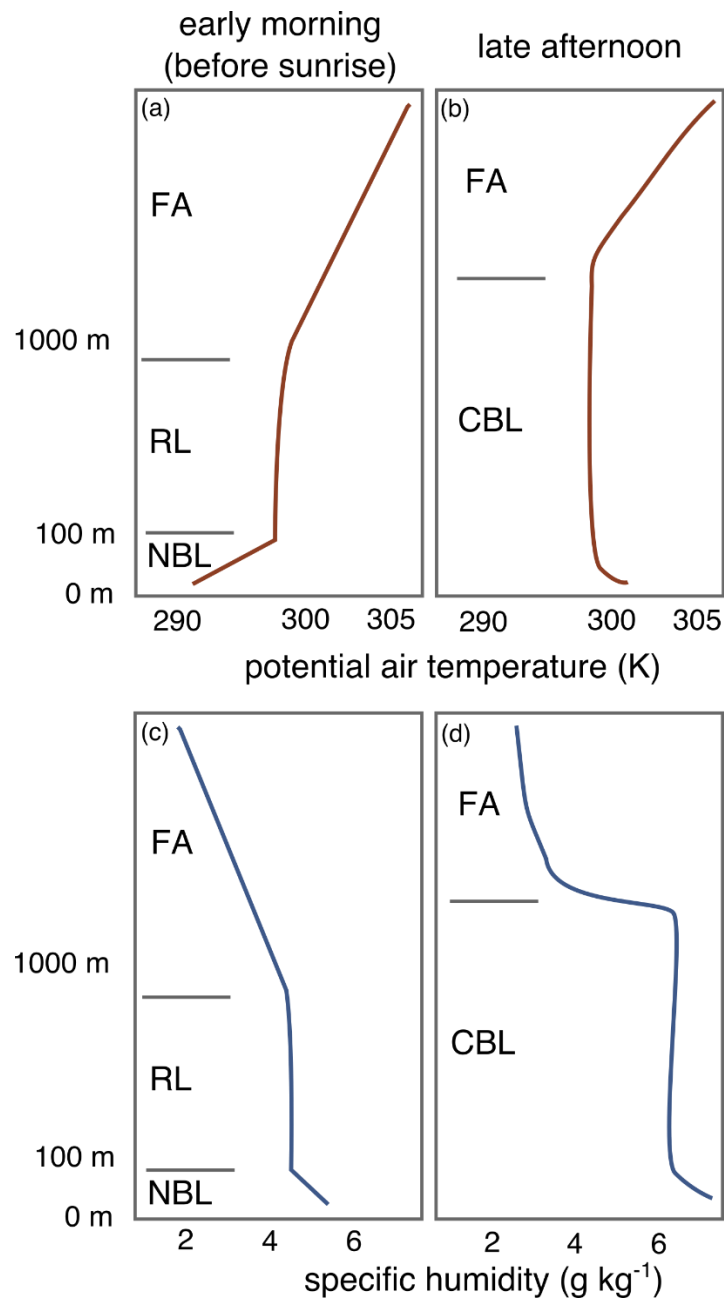
Fig. 3: Typical atmospheric boundary layer profiles of (a & b) potential air temperature and (c & d) specific humidity (a & c) in the early morning just before sunrise and (b & d) in the late afternoon. Diurnal changes in atmospheric boundary layer structure are shown to the left of the profiles (FA = free atmosphere, RL = residual layer, NBL = nocturnal boundary layer, CBL = convective boundary layer). Figure adapted from Stull (1988).
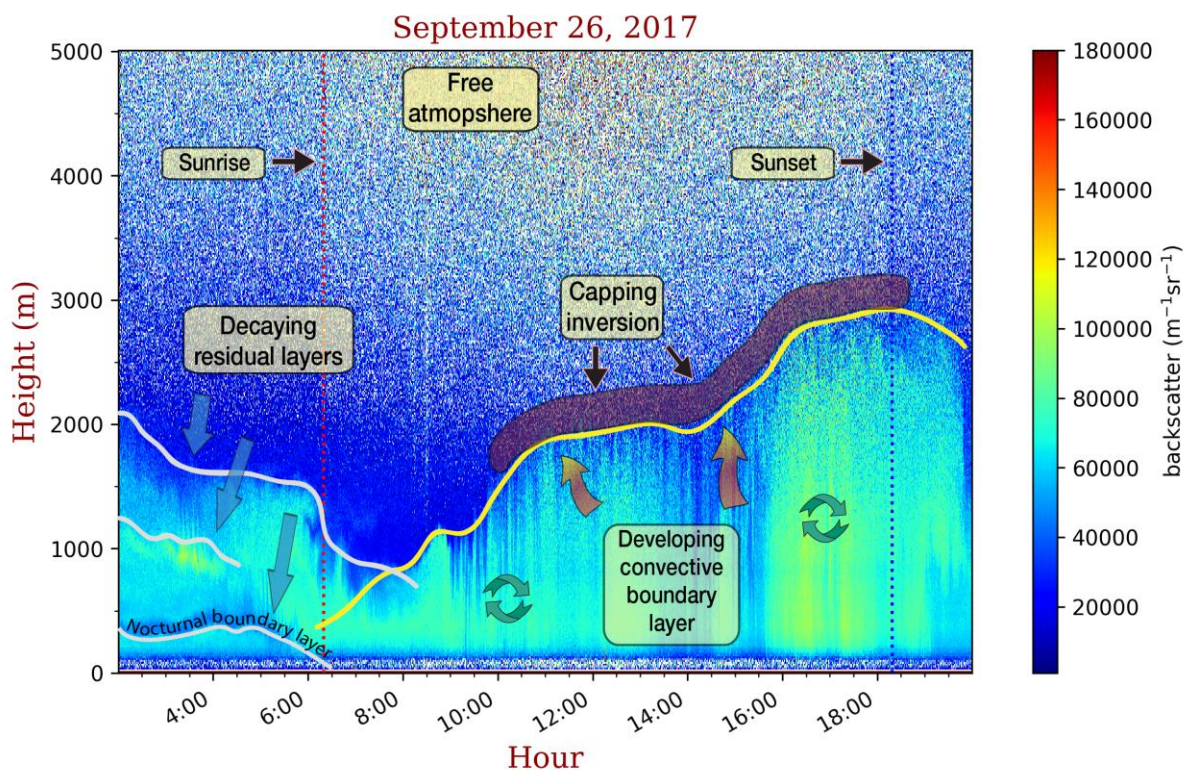
Fig. 4: Example of the diurnal development of a backscatter profile at the USDA-ARS Walnut Gulch Experimental Watershed site in Tombstone, AZ. Colors show the backscatter from a Lufft CHM15k ceilometer between 2:00h and 20:00h. Lines indicate location of the top of the nocturnal boundary layer, residual layer, and convective boundary layer. Vertical dashed lines show timing of sunrise and sunset.

A Doppler Sodar (e.g., radio acoustic sounding system [RASS]) is an acoustic remote sensing instrument. Doppler Sodars derive atmospheric profiles of horizontal and vertical wind velocities and temperature from the scattering of sound pulses (wavelength between 0.1 m and 0.2 m) by atmospheric turbulence (i.e., reflectivity). Vertical reflectivity profiles can be used to derive ABL heights since the interface between ABL and free troposphere (i.e., the entrainment zone) is characterized by intense thermodynamic fluctuations and thus by a maximum in reflectivity (Beyrich, 1997). However, the vertical range of Sodar instruments is typically restricted to heights well below 1000 m. Deep ABLs can therefore not be detected using Sodar technology. Additional constraints of Sodar instruments are related to noise issues to the local community.

Another technology widely used to observe the ABL are wind profiling radars (e.g., Yi et al., 2001) and lidars (e.g., Tucker et al., 2009). Wind profiling radars emit pulses of electromagnetic radiation (wavelength of ~0.5 m) along one vertical beam and two to four oblique beams, and receive backscatter signals, which can be used to derive atmospheric profiles of wind speed and direction. Radar wind profilers have a wider vertical range compared to Doppler Sodar systems but typically lack coverage at heights below 100 m in the case of the 915 MHz profiler, and to 500 m

10

when using the 449 MHZ profiler (Table 2). ABL heights can be derived by identifying the maximum signal-to-noise ratio (SNR) in the backscatter, which is proportional to the maximum in the refractive-index structure parameter (Wesely, 1976; White et al., 1991). This maximum typically coincides with lower humidity levels (Grimsdell & Angevine, 1998; White et al., 1991), buoyancy fluctuations (Angevine et al., 1994; Bianco et al., 2008), and the steepest gradient in air temperature, humidity, and aerosol concentration at the intersection between ABL and free troposphere (Compton et al., 2013; Molod et al., 2015). A continuous time series of ABL height can be obtained after careful processing of the data, which includes range-correction of the signal, filters on atmospheric contamination and spatial and temporal coherence among channels, and the correct selection of peaks along multiple peaks in SNR that can be found along the range of the profiler (e.g. Bianco et al., 2008; Molod et al., 2015). Wind profiling lidars are similar to radars except that they use light instead of radio waves. Due to the use of shorter wavelengths, these lidars can also pick up the movement of aerosols with air motions (Grund et al., 2001). In comparison to wind profiling radars, lidars can resolve shallow ABLH (e.g., Tucker et al., 2009).

Tab. 2: Available technologies for ground-based atmospheric boundary layer observations and specifications of selected individual instruments. Note that price estimates are approximate and may be subject to change. Specifications and basic information on instruments have been sourced from manufacturer websites.

Ceilometers	Price	Wavelength	Pulse Freq (Length)	Power	Vertical Range	Temporal Res.	Vertical Res.	Height (Weight)	MLH/PBL	Basic Information
Campbell CS135	$26,000 USD	905 nm	10 kHz (100 ns)	470 W (max)	10 km	2 - 600 sec	5 meters	1 m (33 kg)	MLH (Gradient)	High signal-to-noise ratio, high detector sensitivity, and single-lens design
Lufft CHM 15k NIMBUS	$28,000 USD	1064 nm	5 - 7 kHz (1 ns)	450 W (max)	15 km	2 - 600 sec	5 meters	0.5 m (70 kg)	PBL (MXL)	Rugged ceilometer with heating and cooling system, able to withstand extreme conditions
PSI Compact Ceilometer	Production model price TBD	1550 nm	3 ns	20 W (typical)	12 km	30 sec	30 meters	0.25 m (10 kg)	MLH	Compact ceilometer requiring minimal power, with the ability to be mounted on flux towers
MiniMPL-532-C (Micro Pulse)	$120,000 USD	532 nm	2.5 kHz (15 ns)	100 W (typical)	15 km	1 - 900 sec	5 meters	0.5 m (13 kg)	PBL	Compact instrument designed to operate in controlled environments with a high signal-to-noise ratio and dual polarization backscatter
Vaisala CL51 Ceilometer	$38,000 USD	910 nm	6.5 kHz (100 ns)	310 W (typical)	15 km	6 - 120 sec	10 meters	1.5 m (46 kg)	MLH (Gradient)	Designed to measure high-range cirrus clouds without missing low and middle cloud layers
Vaisala CL31 Ceilometer	$32,000 USD	910 nm	10 kHz (100 ns)	310 W (typical)	7.7 km	2 - 120 sec	10 meters	1.2 m (31 kg)	MLH (Gradient)	Fast measurements enable the ceilometer to detect thin cloud layers below solid cloud bases
ICOS Leosphere ALS 300	--	355 nm	20 Hz (5 ns)	750 W (max)	15 km	10 - 30 sec	15 meters	1.2 m (36 kg)	PBL	Furnished with an advanced inversion layer detection algorithm, this LiDAR system detects and classifies PBL layers in real time

Balloon Soundings	Price	Power	Vertical Range	Temporal Res.	Weight	Basic Information
Windsond (incl. ground station)	$5,000	100 mW (max)	8 km	1 second	13 grams	Small, recoverable, and reusable sondes reporting real-time wind, temperature, and humidity profiles.
Vaisala RS41 Radiosonde (excl. ground station)	~$120 each	60 mW (min)	~30 - 40 km	1 second	109 grams	Radiosonde used to streamline launch preparations, reduce human errors, and lower operational costs
Vaisala RS92-NGP & LMS-06 (NWS) (excl. ground station)	~$325 each	60 mW (min)	~30 - 40 km	1 second	250 - 500 grams	Since the late 1930s, the NWS has taken upper air observations (0 – 7 km) by use of radiosondes. Rawinsondes measure the typical radiosonde measurements (Pa, Ta, and RH) plus winds.

Doppler Sodar	Pulse Freq (Length)	Vertical Range	Temporal Res.	Vertical Res.	Basic Information
Mini-Doppler Sodar-RASS DSDPA.90-24	SODAR: 1598 Hz (100 ms) RASS: 2897 Hz (100 ms)	400 - 600 meters	10 - 20 seconds	5 - 20 meters	Measures vertical wind profiles and (virtual) temperature between the surface and 600 m. The Sodar (Sonic Detection and Ranging)/RASS (Radio Acoustic Sounding System) transmits acoustic pulses upward, providing reference ABL heights and/or the profiles of turbulent fluxes from reflected pulses

Atmospheric boundary layer measurements

Radar Wind Profiler	Wavelength		Frequency	Power	Vertical Range	Temporal Res.	Vertical Res.	Wind Res.	Basic Information
915 MHz Radar Wind Profiler (Vaisala LAP3000)	0.33	meters	Radar: 915 MHz RASS: 2000 Hz	400 - 600 W (max)	2 - 5 km	Vertical: 1 - 2 min Horizontal: 15 - 30 min	Low: 60 & 100 m High: 250 & 500 m	Speed: ~1 m/s Direction: ~ 5 degs	Fixed ultra-high frequency radars designed to measures wind and precipitation profiles through the boundary layer. More affordable and smaller to build and operate than a 404 MHz (NPN) profiler
449 MHz Radar Wind Profiler	0.67	meters	449 MHz	2000 W (max)	8 - 10 km	30 s - 5 min	~100 m	--	All-weather modular wind profiler able to observe winds and turbulence profiles in the lower atmosphere even under clear skies with little or no water vapor (moisture) present. The 1/4 scale profiler combines the best sampling attributes of other systems.

Lidar Wind Profiler	Wavelength	Pulse Freq	Power	Vertical Range	Temporal Res.	Vertical Res.	Wind Res.	Basic Information
WindTracer (Lockheed Martin)	1,617 nm	500 - 700 Hz	10,000 W	15 km	-	45 - 56 m	< 1 m/s	Measurement technique based on the Doppler Effect allows for the tracking of moving objects (e.g., aerosols) and a depiction of wind fields
HALO Photonics Streamline Wind Lidar	1,500 nm	15,000 Hz	130 W	12 km	1.67 s	30 m	< 0.1 m/s	Compact, lightweight, and portable sampling Doppler LiDAR system with low power consumption
NOAA High-Resolution Doppler Lidar	2,022 nm	200 Hz	-	Typically 3 km Max: 9 km	0.02 s	30 m	0.05 m/s	Measures and maps atmospheric velocities and backscatter with high precision and sampling rates necessary for boundary layer studies

4. Previous and ongoing ABL observations co-located with eddy covariance flux instrumentation

To date, there have been relatively few instances of continuous, high-frequency atmospheric measurements of ABLH being conducted simultaneously with co-located eddy covariance flux measurements (Table 3) and ABLH observations are not routinely shared in the AmeriFlux database. Until a Vaisala ceilometer was installed at the Morgan Monroe State Forest AmeriFlux site in 2006, it appears that previous efforts had been limited to campaigns only a few months to one year in duration. For example, in 1999, one year of atmospheric boundary layer profile measurements were measured at the Walker Branch Watershed (US-Wbw). The Morgan Monroe measurements were discontinued in 2013. Currently, there are ongoing, long-term ABLH measurements at (or near) six AmeriFlux sites (US-SGP, US-A03, US-A10, US-Ho1, US-KFS, US-Wkg, US-Tw1, US-Tw3). The US-SGP, US-A03, and US-A10 measurements are collected as part of the DOE ARM program (www.arm.gov), while the US-Twt1 and US-Tw3 measurements are collected through the NOAA ESRL program. The measurements at US-Ho1 were initiated by the site PI, while those at US-Wkg and US-KFS were initiated by site collaborators. Campaigns on NBLs were conducted at the Tonzi (US-Ton) and Wind River (US-WRC) sites (Wharton et al., 2017). At the 47 NEON terrestrial sites, neither ceilometers nor wind profilers are included in the instrument package deployed. In Europe, the ICOS network is planning to deploy ceilometers at all Class 1 atmospheric monitoring stations, but instrument specifications and operation protocols are still under development. Three sites of the TERENO pre-Alpine observatory in Germany are equipped with ceilometers for ABLH detection since 2012 (sites DE-Fen, DE-RbW, and DE-Gwg; Eder et al., 2015; Kiese et al., 2018).

Tab. 3: Examples of previous and ongoing atmospheric boundary layer observations co-located with eddy covariance flux towers. Links to publications and additional information on the flux tower sites can be accessed through the footnotes.

Location	Site Code	Contact	Measurements	Period	Instrument(s)
Walker Branch, TN[1]	US-WBW	K. Davis & D. Baldocchi	boundary layer height, wind profiles, radar reflectivity	1999	NCAR Integrated Sounding System
Park Falls, WI[1]	US-PFa	K. Davis	boundary layer height, wind profiles, radar reflectivity	1998-99	NCAR Integrated Sounding System
Old Jack Pine, SK (BOREAS)[2]	CA-Ojp	J. Wilczak	boundary layer height	1994	NOAA/ETL 915 MHz radar wind/RASS profiler
Morgan Monroe State Forest, IN[3]	US-MMS	K. Novick	boundary layer height, cloud base and amount; backscatter profile	2006-09, 2011-13	Vaisala CL31 lidar ceilometer
Southern Great Plains ARM, OK[4]	US-SGP	DOE ARM	boundary layer height, cloud base and amount; backscatter profile; wind profiles;	2011-	CEIL lidar ceilometer; radar wind profiler; micropulse lidar
Utqiaġvik, AK[5]	US-A10	R. Sullivan	boundary layer height, cloud base and amount, water vapor, temperature, and turbulence profiles	2011-	Ceilometer, micropulse lidar, balloon sonde, G-band radiometer profiler, microwave radiometer
Tonzi, CA[6]	US-Ton	S. Wharton & D. Baldocchi	wind profile from ground to 150m, thermodynamic and wind profiles from ground to top of troposphere, PBL height	2012-13	WindCube v2, ZephIR 300, radiosondes
Howland Forest, ME	US-Ho1	D. Hollinger	boundary layer height, cloud base and amount; backscatter profile	2013-	Vaisala CL31 lidar ceilometer
INFLUX (Indianapolis Flux Experiment)[7]	-	K. Davis	boundary layer height, wind profiles	2013-15	Scanning doppler lidar
Oliktok Point, AK[5]	US-A03	R. Sullivan	boundary layer height, cloud base and amount, water vapor, temperature, and turbulence profiles	2014-	Ceilometer, micropulse lidar, balloon sonde, radar wind profiler, Doppler lidar
Walnut Gulch, AZ	US-Wkg/Whs	J. Perkins & P. Hazenberg	boundary layer height, cloud base and amount; backscatter profile	2017-	Lufft CHM15k lidar ceilometer
Walnut Gulch, AZ	US-Wkg/Whs	A. Richardson	boundary layer height, cloud base and amount; backscatter profile	2019-	Campbell CS135 lidar ceilometer
CHEESEHEAD19, WI[8]	US-PFa	A. Desai	boundary layer height, cloud base, aerosol backscatter and polarization, PBL temperature, wind	June-Oct 2019	NCAR Integrated Sounding System, UW SSEC SPARC (AERI AND HSRL), KIT IFU

Atmospheric boundary layer measurements

Site	Code	PI	Measurements	Dates	Instruments
			and moisture profiles, radar reflectivity, precipitation imaging		H2O and wind LiDAR, NOAA CLAMPS and SURFRAD, UW MRR and PIP
Twitchell Island, CA[9]	US-Twt	D. Baldocchi & NOAA	boundary layer sounding	2017-	915 MHz wind profiler
Kansas Field Station, KS[10]	US-KFS	N. Brunsell	boundary layer height, cloud base and amount; backscatter profile	2017-	Vaisala CL31 lidar ceilometer
Graswang, Germany[11]	DE-Gwg	M. Mauder (TERENO)	boundary layer height, cloud base and amount; backscatter profile	2012-	Vaisala CL51 lidar ceilometer
Rottenbuch, Germany[11]	DE-RbW	M. Mauder (TERENO)	boundary layer height, cloud base and amount; backscatter profile	2012-	Vaisala CL51 lidar ceilometer
Fendt, Germany[11]	DE-Fen	M. Mauder (TERENO)	boundary layer height, cloud base and amount; backscatter profile	2012-	Vaisala CL51 lidar ceilometer
NY State Mesonet (17 sites, co-located atmos. & eddy covariance measurements)[12]	-	C. Thorncroft	atmospheric profiles: winds up to 7km above the surface; temperature and liquid up to 10km above the surface	2018-	Leosphere WindCube WLS-100 series Doppler LiDAR; Radiometrics MP-3000A Microwave Radiometer
Ruisdael Obs., Netherlands[13]	multiple	H. Russchenberg	various	in dev.	multiple instruments for in situ characterization of physical and chemical properties of the atmosphere
Tapajos National Forest, Brazil	BR-SA1	S. Saleska & S. Wofsy	cloud base, backscatter profile	2001-03	Vaisala CT-25K ceilometer

[1]https://www.osti.gov/biblio/808114-regional-forest-abl-coupling-influence-co-sub-climate-progress-date; [2]https://daac.ornl.gov/cgi-bin/dsviewer.pl?ds_id=240 ;
[3]https://www.sciencedirect.com/science/article/pii/S0168192311000244; [4]https://www.arm.gov/capabilities/observatories/sgp; [5]https://www.arm.gov/capabilities/observatories/nsa;
[6]https://www.sciencedirect.com/science/article/pii/S0168192317300308; [7]https://sites.psu.edu/influx/; [8]https://www.eol.ucar.edu/field_projects/cheesehead;
[9]https://www.esrl.noaa.gov/psd/data/obs/sites/view_site_details.php?siteID=tci; [10]https://ameriflux.lbl.gov/sites/siteinfo/US-KFS; [11]https://www.tereno.net; [12]http://nysmesonet.org/about/welcome; [13]http://ruisdael-observatory.nl/

5. Research opportunities emerging from co-located ABL and tower-based surface flux observations at AmeriFlux sites

Extending current ABL observations across the AmeriFlux network would open new opportunities to tackle pressing research questions and add value and exposure to ongoing eddy covariance flux measurements. In this section, we outline how continuous and long-term ABL observations at flux tower sites would provide crucial information to (1) interpret surface flux dynamics at AmeriFlux sites, (2) support regional-scale modelling and upscaling of surface fluxes, (3) validate land-atmosphere coupling in Earth system models, and (4) support flux footprint modelling and quality control of flux measurements (including flux correction algorithms).

5.1. Interpretation of surface flux measurements

To fully understand the coupling between surface fluxes and atmosphere, ABL height observations in addition to eddy covariance flux measurements are required. Fluxes of mass and energy at the land surface, as measured at eddy covariance tower sites, are not isolated from the conditions of ABL and free troposphere. Mass and energy fluxes at the land surface respond to changes in ABL depth and to the heat, moisture, and matter that is mixed into the growing ABL from the free troposphere (i.e., entrainment). In turn, the depth of the ABL and the concentration of scalars within it are a function of the surface fluxes and the entrainment of dry air from above the growing ABL (Denmead et al., 1996). Thus, observations of ABL conditions and of its growth can support the interpretation of surface flux observations.

The growth of the ABL is directly coupled to land surface conditions and is influenced by feedback mechanisms between the surface energy balance and the entrainment of dry and warm air from above ABL. Entrainment can present a negative feedback as drier air increases latent heat exchange and reduces sensible heat exchange and thus slows down ABL growth (e.g., McNaughton & Spriggs, 1986; Salvucci & Gentine, 2013). However, closing of the stomata in response to increasing vapor pressure deficit reduces leaf surface conductance and can sometimes result in an increase in sensible heat at the expense of latent heat flux (i.e., increasing Bowen ratio; Helbig et al., 2020; Lansu et al., 2020; Fig. 2). In addition, cloud formation and precipitation occurrence are tightly coupled to ABL growth dynamics (Konings et al., 2010). If the ABL height reaches the LCL, condensation occurs, and convective clouds may form. Cloud formation reduces the amount of solar radiation that reaches the Earth's surface (Juang et al., 2007; Vilà-Guerau de Arellano et al., 2014), and reduced available energy at the land surface can exert a negative feedback on surface energy fluxes and photosynthesis. However, the increase in diffuse radiation can also positively affect photosynthetic uptake (Knohl & Baldocchi, 2008).

Surface fluxes are directly influenced by atmospheric stability via turbulence and mixing and, thus, atmospheric profile measurements of temperature and wind (i.e., measurements needed to derive atmospheric stability) may improve our understanding of atmospheric driving mechanisms of surface fluxes. For example, aerodynamic coupling between land surface and ABL affects the surface energy balance through an effect on atmospheric stability. During unstable conditions, a negative feedback occurs: an increase in surface temperature increases convective instability, turbulent mixing, and aerodynamic conductance, resulting in an increase in sensible heat flux. This increase in sensible heat flux acts to reduce surface temperature. During stable atmospheric conditions, temperature profiles are inverted, and turbulence is dampened. Over well-watered surfaces, the downward transport of sensible heat feeds evaporation and evaporative cooling of the surface reinforcing the temperature inversion and promoting further stable stratification (Brakke et al., 1978; Lang et al., 1974, 1983).

The ABL height represents the vertical extent of the region, where the atmosphere is directly influenced by the Earth's surface. Therefore, the ABL height has been used as an outer-layer scaling parameter under a range of atmospheric stability conditions (Zilitinkevich et al., 2012, Banerjee and Katul, 2013, Banerjee et al., 2014, Banerjee et al, 2015) to describe the exchange between the land surface and the atmosphere. The measurement of ABL height alongside land-atmosphere flux exchange can help constrain surfaceflux measurements. On the other hand, the ABL height itself is a function of the sensible heat flux gradient across the boundary layer. Under planar and homogeneous conditions, the ABL height can be computed by a thermodynamic encroachment model:

$$\frac{dh}{dt} = \frac{\overline{w'\theta'} - \overline{w'\theta_h'}}{\gamma\, h}$$

where h is the ABL height, $\overline{w'\theta'}$ is the kinematic sensible heat flux at the surface, $\overline{w'\theta_h'}$ is the entrainment flux at the ABL top, and γ denotes the potential temperature gradient of the free atmosphere above the ABL (Zilitinkevich et al., 2012; Brugger et al., 2018). The entrainment heat flux can be modeled as a fixed proportion of the surface heat flux. This model approximates the ABL as a single slab without any internal source and sink terms. Integrating this equation offers a technique to couple turbulent flux measurements with the eddy covariance method and ABL observation at a particular site (Brugger et al., 2018).

In addition, understanding ABL dynamics is key to understanding regional scale evaporation (McNaughton & Spriggs, 1986; van Heerwaarden et al., 2009), carbon budgets (Betts et al., 2004; Denmead et al., 1996), atmospheric chemistry (Vilà-Guerau de Arellano et al., 2011), and greenhouse gas flux dynamics (Zhao et al., 2009). The land surface-ABL couplings can establish a set of explanations for scale emergent observations and practical applications. Examples for such

applications include: (1) establishing the upper limit on regional latent heat exchanges and, thus, water loss to the atmosphere; (2) using the atmosphere as a soil moisture sensor through the interpretation of feedbacks between vapor pressure deficits and soil moisture; (3) quantifying the partitioning of the net ecosystem exchange between plant assimilation and soil respiration.

Finally, the profiles of wind and air temperature in the lowest levels of the ABL (i.e., the roughness sublayer, the surface layer, and into the lower mixed layer) can provide critical information for extrapolating the influence of vegetation structure and function at the surface into the ABL. In the surface layer, wind and temperature profiles are often well-described as logarithmic functions of height (i.e., Monin-Obuhkov Similarity Theory functions for the diabatic profiles of wind and temperature, Monin & Obukhov, 1954). The parameters of these functions depend on fluxes measured by towers (e.g., momentum and sensible heat), as well as scaling parameters like the zero-plane displacement and roughness lengths for momentum and heat (which themselves are strongly affected by canopy structure, Brutsaert 1982). Properly constraining the parameters of these profile equations is made substantially easier if at least one, and ideally multiple, observations of the key scalars (air temperature, wind speed) are made within the surface layer, which is often assumed to begin at a height of 2-5 times the height of the canopy (Raupach & Thom, 1981). For short stature ecosystems (i.e. grasslands, croplands) with canopy heights <1 m, many existing flux tower heights extend into the surface layer, substantially facilitating the application of similarity theory. However, for forests and woodlands, most flux towers heights are constrained to within the roughness sublayer, where diabatic profile functions do not apply due to local, near-surface canopy drag effects. In these sites, additional information about the profiles of temperature and wind in the surface layer (for example, from balloon soundings or sodar) could better constrain estimates of the zero-plane displacement and roughness lengths, and better facilitate the transfer of information about measured fluxes to their impacts on atmospheric state variables throughout the ABL (e.g., Novick & Katul, 2020).

ABL growth observations can help interpret differences in measured evaporation rates over a spectrum of sites from well-watered and productive to dry, sparse and unproductive. Evaporation of an extended wet surface exceeds the equilibrium rate of evaporation (lE_{eq}) through the coupling mechanisms between land surface and ABL. The ratio between actual evaporation and lE_{eq} approaches the value of the Priestley-Taylor coefficient (i.e., 1.26; Priestley & Taylor, 1972). This effect can be best demonstrated by applying a coupled ABL model (McNaughton & Spriggs, 1986) that links the Penman-Monteith equation to a simple one-dimensional slab ABL model. Evaporation rates depend on the vapor pressure deficit within the ABL, whose growth and entrainment depend on sensible heat flux at the surface (e.g., Raupach, 2000, 2001). Under conditions of low surface resistance (i.e., well-watered conditions), the ratio of actual evaporation to lE_{eq} approaches 1.26 as a

result of this coupling. If well-watered surfaces are isolated within a drier landscape, large sensible heat flux and enhanced vapor pressure deficit can accelerate water losses to the atmosphere and lead to ratios of actual evaporation to IE_{eq} well above 1.26 (Shuttleworth et al., 2009; Baldocchi et al., 2016).

Observations of atmospheric temperature and humidity profiles and ABL growth across AmeriFlux sites can provide unique datasets to validate novel techniques to estimate regional evaporation rates (e.g., Rigden & Salvucci, 2015). One of the outstanding challenges to computing land atmosphere fluxes is assessing the down regulation of stomatal (and surface) conductance as soil moisture deficits increase (Fig. 2). The lack of consistent and large-scale soil moisture observations poses another challenge to this task. Recent work has demonstrated how plants can act as a sensor for soil moisture and has detected their influence on the humidification of the ABL (e.g., Pedruzo-Bagazgoitia et al., 2017; Vilà-Guerau de Arellano et al., 2014). The vertical variance of the relative humidity profile within the ABL can be used to infer the large-scale surface conductance from weather station data only (Gentine et al., 2016; Salvucci & Gentine, 2013). Due to the tight coupling of latent heat exchange at the land surface and atmospheric humidity and temperature, these approaches can serve as an inferential measure of land surface conditions (e.g., soil moisture) at large spatial scales (McColl & Rigden, 2020) and have been used successfully to compute evapotranspiration rates across North America (Rigden & Salvucci, 2015) and to understand the role of plants in regulating droughts/extreme heat wave events (Combe et al., 2016)

Analyses of land use and cover impacts on near-surface climates can be expanded across Ameriflux, but require both direct ABL measurements and models to interpret observations. Recent work at AmeriFlux sites has assessed how land use and cover affects local air temperatures through land surface-atmosphere interactions (Baldocchi & Ma, 2013; Helbig et al., 2016; Hemes et al., 2018; Novick & Katul, 2020). To quantify such effects on local near-surface and regional climate, the coupling between land surface, ABL, and free troposphere has to be accounted for (van Heerwaarden et al., 2009). Coupled ABL models can be used in this context. However, ground observations of ABL height and sounding profiles remain critical to further validate these models. Similarly, co-location of flux towers and ABL observations in urban environments can help better understand the effect of urban planning on near-surface climate and air pollution and thus on human health and comfort (e.g., Kotthaus & Grimmond, 2018b; Wood et al., 2013).

Apart from surface heating and cooling, the ABL height is also highly sensitive to land surface cover, topography, and synoptic conditions. While a number of studies have investigated the changes in ABL height with atmospheric stratification, studies on the impact of surface heterogeneity and land-cover transitions on ABL height are scarce. Brugger et al. (2018) investigated the influence of surface

heterogeneity on ABL height in the context of a semi-arid forest surrounded by a shrubland (i.e., Yatir forest in the Negev desert, Israel). The presence of a large scale surface heterogeneity violated the assumption of planar homogeneous conditions; however, an internal boundary layer model originally conceptualized by Venkatram (1977) and modified by Brugger et al. (2018) was used to compute the change of ABL height due to the surface roughness transition. This model accounts for turbulent fluxes measured by eddy covariance towers over the different surfaces and the geometric configuration of the transition, and couples these measurements with the mixed layer and ABL measurements over the land surfaces. For example, a transition from a shrubland to forest results in the growth of an internal boundary layer, which assumes a vertical transport of the forest's effects at the convective velocity scale to the ABL top while being advected horizontally at the same time by the background flow. Kröeniger et al. (2018) conducted large eddy simulation over the same site and was able to validate this model and the eddy covariance measurements along with ABL models were useful to interpret the results, especially to investigate the role of secondary circulations that could further modulate land-atmosphere exchange (Banerjee et al., 2018). Similar modeling exercises reinforced with co-located eddy flux and ABL measurements could be beneficial for other applications such as models for regional climate, pollutant transport, and urban heat islands.

5.2 Regional scale modeling and forward transport and dispersion models

Atmospheric boundary layer height measurements can be used with additional concentration measurements to infer regional budgets of conserved scalars such as carbon dioxide or methane (Wang et al., 2007; Wofsy et al., 1988; Yi et al., 2004). Raupach et al. (1992) describe the CBL budget approach that assumes the bulk of the ABL is well mixed, the surface layer (affected by surface fluxes) is thin, and that the ABL height growth is rapid in comparison to subsidence from the atmosphere above (see also Betts, 1992). These conditions may occur during the middle of sunny clear days when high pressure systems are dominant. Under these circumstances,

$$\frac{dC_m}{dt} = \frac{F_c}{h} + \left(\frac{C_+ - C_m}{h}\right)\frac{dh}{dt}$$

Where C_m is the average concentration of the scalar C throughout the well-mixed CBL, h is the boundary layer depth, C_+ is the concentration of the scalar in the free atmosphere just above the CBL (height h), and F_C is the surface flux of the scalar. For example, Denmead et al. (1996) used this conservation equation in both differential and integral form to estimate regional water vapor and carbon dioxide flux over agricultural land. Furthermore, the convective budgeting approach was used in other regional budget studies such as FIFE (Betts & Ball, 1994), BOREAS (Barr & Betts, 1997), and at AmeriFlux tall tower sites (Desai et al., 2010; Helliker et al.,

2004). Cleugh & Grimmond (2001) tested and refined this approach over a mixed (rural to urban) landscape, while Baldocchi et al. (2012) used atmospheric budgeting to better understand anomalies in methane fluxes.

Denmead et al. (1996) also discussed the potentially simpler issue of NBL budgeting. During nights with strong temperature inversions, the boundary layer collapses to heights of only tens of meters, trapping surface emissions in a shallow layer. Monitoring the time rate of change of a scalar (C) through the inversion to height h yields a flux (F_C),

$$F_c = \int_0^h \frac{dC}{dt} dh$$

Note that it is just during these stable, nocturnal periods characterized by an absence of turbulence, when the eddy covariance method fails. The NBL budget method was first used with tethered balloons carrying sampling tubes leading to a ground-based analyzer (e.g., Choularton et al., 1995). The rapid advance of small UAVs and their use in carrying CO_2 and other equipment for atmospheric measurement (e.g., Brady et al., 2016) suggest many new opportunities for the NBL budget method.

Inverse atmospheric transport modeling approaches require ABL height, although typically modeled values have been used instead of measured heights. Inverse atmospheric transport modeling approaches combine ABL concentrations of scalars (measured most often by aircraft) with wind fields from mesoscale models and have superseded in many instances the CBL budget approach for inferring regional surface fluxes. Many of these methods such as the Stochastic Time-Inverted Lagrangian Transport (STILT) model (Lin et al., 2003) have grown from NOAA HYSPLIT atmospheric transport and dispersion modeling system (see Stein et al., 2015 for a review). An advantage of this approach is the explicit calculation of upwind source areas as well as surface fluxes. Inverse modeling approaches have recently been used, for example, in studies of methane emissions from northern regions (Hartery et al., 2018). Similarly, global or regional inversion systems aimed at constraining terrestrial carbon budgets can assimilate carbon dioxide observations from a variety of sources, including towers, aircrafts, and total column measurements using satellites (such as the Orbiting Carbon Observatory/ OCO-2) but remain sensitive to transport model error and the strength of vertical mixing, which is directly related to ABL evolution and height (Basu et al., 2018; Lauvaux & Davis, 2014; McGrath-Spangler et al., 2015).

5.3 Land-atmosphere coupling and model validation

The combination of ground-based observations of surface fluxes (e.g., eddy covariance or scintillometry) and observations of ABL (or mixed layer) height

allow for closure of ABL energy, water, and gas budgets and can therefore serve as a tool for validation of atmospheric models. Land-atmosphere interactions lead to coupling between land and atmosphere, which can mediate feedback in weather and climate (e.g., Santanello et al., 2017). For example, ABL heating and drying leads to higher evaporative demand from vegetation and soils through higher vapor pressure deficit (VPD). Under well-watered conditions (i.e., with sufficiently high soil moisture), latent heat exchange increases, which in turn moistens the ABL (Santanello et al., 2017; Seneviratne et al., 2010; van Heerwaarden et al., 2009), while subsequently decreasing soil moisture. Lower soil moisture is associated with higher sensible and lower latent heat fluxes and thus enhanced ABL growth and further warming (e.g., Sanchez-Mejia & Papuga, 2014, 2017). Such feedbacks - highly variable in space and time - are difficult to observe (Gerken et al., 2019; Koster et al., 2009) thus limiting our atmospheric process understanding (e.g., Betts, 2009; Ek & Holtslag, 2004; Santanello et al., 2017).

Combining continuous and distributed observations of ABL height with turbulent fluxes would help to better validate land-atmosphere modeling efforts and to better quantify the sensitivities of the land-atmosphere system to ABL height growth dynamics across the biomes represented in the AmeriFlux network. Models of various complexity and scales (including slab, single-column, large-eddy simulation, regional, and Earth system models) have been used to increase our understanding of land-atmosphere coupling and feedback. Slab-type models, which only require estimates of the diurnal cycle of sensible and latent heat fluxes as well as atmospheric temperature and moisture lapse rates, have been commonly used to understand timing and onset conditions of ABL clouds or local convective precipitation (e.g., Gentine et al., 2013a; Gentine et al., 2013b; Gerken et al., 2018; Juang et al., 2007; Juang et al., 2007; Manoli et al., 2016) and have also been extended to include carbon and other atmospheric trace gases at the center of land-atmosphere interactions (e.g., Vila-Guerau de Arellano et al., 2015). Observations of ABLH could be used to validate these models to better understand the role of land cover, use, and management in ABL dynamics (e.g., Helbig et al., 2016; Luyssaert et al., 2014; Vick et al., 2016). In addition, the observations of ABLH and associated gradients of temperature, humidity, and wind speed can be assimilated in numerical models to improve weather forecasting. Resulting datasets can be used to verify the fidelity of outputs from numerical models.

Flux tower sites with continuous ABL observations could expand on the idea of test-bed sites such as the U.S. Department of Energy (DOE) Atmospheric Radiation Measurement (ARM) user facility sites with the LASSO (Large-Eddy Simulation ARM Symbiotic Simulation and Observation) project (Gustafson et al., 2020) or the Royal Netherlands Meteorological Institute Parameterization Testbed (Neggers et al., 2012) that integrates observations with LES, slab models and operational models. In this context, observations could be used to diagnose entrainment fluxes of water, energy, and atmospheric trace gases at the ABL top

(Santanello et al., 2011) or to elucidate the surface and atmospheric controls on convective precipitation over wet and dry soils (e.g., Findell & Eltahir, 2003a, 2003b; Ford et al., 2015; Yin et al., 2015). Recently, the role of land-atmosphere feedbacks for expansion and intensification of droughts and heatwaves has been highlighted (Miralles et al., 2014, 2019). Given the importance of droughts and heatwaves for the carbon cycle (Wolf et al., 2016), water resource and wildfire management, agriculture, and human health, the combined flux and ABL height observations across the AmeriFlux network have the potential to contribute to better quantification of these feedback processes, arising from cumulative drying of soils, increased surface flux partitioning toward sensible heat flux, and subsequent heat accumulation in the ABL (Miralles et al., 2014).

Future studies within the AmeriFlux network need to go beyond the ecosystem scale and address the interdisciplinary aspects of land-atmosphere interactions and connect spatiotemporal scales. In that respect, the short and long-term responses of vegetation to the dynamics of clear and cloudy boundary layers are still an open issue. Tackling this land-atmosphere interaction could help to reduce two large uncertainties in climate change: the coupling of terrestrial uptake of carbon dioxide and boundary-layer clouds, including their transitions. At sub-diurnal and sub-kilometer scales, it is necessary to further quantify how vegetation controls the partitioning between sensible and latent heat flux (Vilà-Guerau de Arellano et al., 2012) and the impact on the cloud cycle (Sikma & Arellano, 2019). Flux tower clusters with multiple flux and ABL observation systems can provide important information on the effect of spatio-temporal variability of surface fluxes and ABL heights on regional land-atmosphere interactions (e.g., Beyrich et al., 2006; Xu et al., 2020). These observational studies will require dedicated observations of ABL growth dynamics, of stable isotopologues (Griffis et al., 2007), and of the partitioning of direct and diffuse radiation (Pedruzo-Bagazgoitia et al., 2017) to identify complex interactions between photosynthesis, evapotranspiration, and cloud cover dynamics.

5.4 Improving quality of eddy covariance flux measurements

Atmospheric boundary layer observations can provide important information on the state of the atmosphere and can thus improve quality control of eddy covariance fluxes. The quality of eddy covariance flux measurements varies with atmospheric conditions and depends on the fulfilment of fundamental micrometeorological assumptions (e.g., negligible advective fluxes). The influence of regional or mesoscale (i.e., non-local) motions on turbulent exchange between the land and atmosphere have often been studied using short-term, campaign-style observations (e.g., Shen & Leclerc, 1995). Such studies revealed the effect of certain ABL processes on uncertainties in eddy covariance flux measurements emphasizing the need for continuous ABL measurements at flux tower sites. These observations could for example detect large vertical exchanges of the canopy airshed, which can originate from the ABL and be important particularly

in tall (e.g., forest) canopies (e.g., Thomas and Foken, 2007; Wharton et al., 2017). Non-local motions can occur at larger timescales than those typically associated with canopy transport and eddy covariance averaging intervals. Patton et al. (2015) argue that single point (e.g., tower) observations should be averaged over time scales of the ABL motions rather than canopy-scale. There is evidence that inability to resolve large eddies that entrain warm-dry air in traditional eddy covariance flux calculation methodology may contribute to the lack of surface energy balance closure, which leads to systematic underestimation of energy and possibly of carbon fluxes at virtually all AmeriFlux sites (Eder et al., 2015; Stoy et al., 2013). Continuous ABL observations of wind speed and direction could be used to identify periods when these eddies are present and be used to correct or flag biased flux measurements (de Roo et al., 2018).

Interpretation of nighttime fluxes is a major focus for the integration of ABL and eddy covariance flux measurements. Friction velocity (u*) thresholds are commonly applied as a proxy for inadequate turbulent mixing whereby periods below the u* thresholds are removed from the estimate of the nighttime carbon dioxide (respiration) flux and subsequently gap-filled. While the appropriateness of u* thresholds remain highly debated (Acevedo et al., 2009), others have focused on understanding the mechanisms for when nocturnal turbulence can be enhanced, particularly by non-local flows (e.g., low-level jets). Wharton et al. (2017) used wind-profiling lidar to identify two different non-local motions (downslope flow and intermittent turbulence) and applied different turbulent parameters for estimating canopy mixing during those periods at two AmeriFlux sites. They found that predicting nocturnal canopy turbulence was a complex interaction of non-local flows and atmospheric stability, which could not be assessed solely by u*. For the case of nocturnal low-level jets, Prabha et al. (2008) invoke a shear-sheltering hypothesis, requiring vertical wind profiles, to differentiate cases when the low-level jet enhanced surface eddy covariance turbulent fluxes at an AmeriFlux site. Without more (and continuous) ABL observations at eddy covariance flux towers, we may bias our nighttime fluxes by over-filtering (e.g., application of u* thresholds). Over-filtering would lead to unnecessary loss of nighttime data and limit our ability to understand dynamics of nighttime fluxes.

Continuous measurements of ABL height dynamics co-located with eddy covariance flux measurements could reduce uncertainties in current flux footprint estimates and thereby help identifying source and sink hotspots at flux tower sites. Flux footprint models provide an important tool to determine the location and extent of the source area of eddy covariance flux measurements, to identify heterogeneous greenhouse gas sources and sinks within the source area, and to improve interpretation of their impact on the measured fluxes (Barcza et al., 2009; Griebel et al., 2016; Vesala et al., 2008; Xu et al., 2017). Footprint estimates either directly (via input parameter) or indirectly (via mixing volume or model validity) depend on the ABL height (Kljun et al., 2015). This dependence is critical especially

for the case of stable atmospheric conditions due to a shallow ABL that can act as a "lid" for sources-sinks, and because nighttime stable footprints typically extend much longer than the typical convective daytime footprints, thus opening opportunities to interpret greenhouse gas and energy fluxes originating from more distant sources (Baldocchi et al., 2012). However, ABL heights are rarely directly measured or determined at flux tower sites. They are instead estimated for case studies using various modeling approaches (see Kljun et al., 2015; Yi et al., 2001). The ABL depth is also essential for footprint modeling when measurement height is greater than 10% of ABL height, which occurs during early mornings or with very tall towers. Footprint models for these cases have been developed but require ABL height estimates (Kljun et al., 2015; Wang et al., 2006).

Atmospheric boundary layer measurements provide crucial observations to address the pressing research questions discussed above. Many land-atmosphere studies at eddy covariance flux tower sites relied on modeling approaches due to the lack of direct ABL observations (e.g., Baldocchi & Ma, 2013; Helbig et al., 2016; Lansu et al., 2020) or made use of upper air sounding observations that are restricted by limited temporal resolution (e.g., Juang et al., 2007). New measurement technologies that have become available recently now allow to expand continuous, high-frequent ABL observations across the FLUXNET network opening new perspectives on complex feedbacks between the land surface and the atmosphere.

6. Recommendations for actions

We propose that efforts to expand the availability of atmospheric boundary layer observations across the AmeriFlux network, either through new instrument deployments or campaigns to gather previously collected data, would allow the Earth science community to address new emerging research questions and add substantial value to ongoing flux tower measurements. Joint atmospheric ABL and surface flux observations would increase the usability of flux tower observations by the broader research community (e.g. remote sensing, Earth system modelling, atmospheric science communities). Adding ABL measurements to more sites within the AmeriFlux network, spanning a range of ecosystem types, climate zones and terrain, and systematic efforts to make new and existing ABL measurements available from the network platform, would

(1) lead to better understanding of complex feedbacks between surface flux and ABL dynamics,

(2) support efforts to upscale surface fluxes from local to regional scales,

(3) provide essential data for the validation of land-atmosphere coupling in Earth system models, and

(4) support flux footprint modelling, the interpretation of surface fluxes in heterogeneous terrain, and quality control of eddy covariance flux measurements.

There is an urgent need to acquire funding to develop the observational infrastructure, to share best practices among flux tower site teams, and to develop protocols and standardized data formats to enable efficient sharing of ABL data (i.e. ABL height, full profiles, cloud amount and height).

Literature

Acevedo, O. C., Moraes, O. L. L., Degrazia, G. A., Fitzjarrald, D. R., Manzi, A. O., & Campos, J. G. (2009). Is friction velocity the most appropriate scale for correcting nocturnal carbon dioxide fluxes? *Agricultural and Forest Meteorology*, *149*(1), 1–10.

Angevine, W. M., White, A. B., & Avery, S. K. (1994). Boundary-layer depth and entrainment zone characterization with a boundary-layer profiler. *Boundary-Layer Meteorology*, *68*(4), 375–385.

Vilà-Guerau de Arellano, J., Gioli, B., Miglietta, F., Jonker, H. J. J., Baltink, H. K., Hutjes, R. W. A., & Holtslag, A. A. M. (2004). Entrainment process of carbon dioxide in the atmospheric boundary layer. *Journal of Geophysical Research: Atmospheres*, *109,* D18110.

Baldocchi, D., Detto, M., Sonnentag, O., Verfaillie, J., Teh, Y. A., Silver, W., & Kelly, N. M. (2012). The challenges of measuring methane fluxes and concentrations over a peatland pasture. *Agricultural and Forest Meteorology*, *153*, 177–187.

Baldocchi, D., Knox, S., Dronova, I., Verfaillie, J., Oikawa, P., Sturtevant, C., Matthes, J. H., & Detto, M. (2016). The impact of expanding flooded land area on the annual evaporation of rice. *Agricultural and Forest Meteorology*, *223*, 181–193.

Baldocchi, D., & Ma, S. (2013). How will land use affect air temperature in the surface boundary layer? Lessons learned from a comparative study on the energy balance of an oak savanna and annual grassland in California, USA. *Tellus B: Chemical and Physical Meteorology*, *65*(1), 19994.

Banerjee, T., & Katul, G. G. (2013). Logarithmic scaling in the longitudinal velocity variance explained by a spectral budget. *Physics of Fluids*, *25*(12), 125106.

Banerjee, T., Katul, G. G., Salesky, S. T., & Chamecki, M. (2015). Revisiting the formulations for the longitudinal velocity variance in the unstable atmospheric surface layer. *Quarterly Journal of the Royal Meteorological Society*, *141*(690), 1699–1711.

Banerjee, Tirtha, Brugger, P., Roo, F. D., Kröniger, K., Yakir, D., Rotenberg, E., & Mauder, M. (2018). Turbulent transport of energy across a forest and a semiarid shrubland. *Atmospheric Chemistry and Physics*, *18*(13), 10025–10038.

Banerjee, Tirtha, Li, D., Juang, J.-Y., & Katul, G. (2016). A spectral budget model for the longitudinal turbulent velocity in the stable atmospheric surface layer. *Journal of the Atmospheric Sciences*, *73*(1), 145–166.

Barcza, Z., Kern, A., Haszpra, L., & Kljun, N. (2009). Spatial representativeness of tall tower eddy covariance measurements using remote sensing and footprint analysis. *Agricultural and Forest Meteorology*, *149*(5), 795–807.

Barr, A. G., & Betts, A. K. (1997). Radiosonde boundary layer budgets above a boreal forest. *Journal of Geophysical Research: Atmospheres*, *102*(D24), 29205–29212.

Basu, S., Baker, D. F., Chevallier, F., Patra, P. K., Liu, J., & Miller, J. B. (2018). The impact of transport model differences on CO_2 surface flux estimates from OCO-2 retrievals of column average CO_2. *Atmospheric Chemistry and Physics*, *18*(10), 7189–7215.

Batchvarova, E., & Gryning, S.-E. (1991). Applied model for the growth of the daytime mixed layer. *Boundary-Layer Meteorology*, *56*(3), 261–274.

Betts, A. K. (1992). FIFE atmospheric boundary layer budget methods. *Journal of Geophysical Research*, *97*(D17), 18523-18531.

Betts, Alan K. (2009). Land-surface-atmosphere coupling in observations and models. *Journal of Advances in Modeling Earth Systems*, *1*(4), doi:10.3894/JAMES.2009.1.4.

Betts, Alan K., & Ball, J. H. (1994). Budget analysis of FIFE 1987 sonde data. *Journal of Geophysical Research: Atmospheres*, *99*(D2), 3655–3666.

Betts, Alan K., Helliker, B., & Berry, J. (2004). Coupling between CO_2, water vapor, temperature, and radon and their fluxes in an idealized equilibrium boundary layer over land. *Journal of Geophysical Research: Atmospheres*, *109*, D18103.

Beyrich, F. (1997). Mixing height estimation from sodar data — A critical discussion. *Atmospheric Environment*, *31*(23), 3941–3953.

Beyrich, F., Leps, J.-P., Mauder, M., Bange, J., Foken, T., Huneke, S., Lohse, H., Lüdi, A.,

Meijninger, W. M. L., Mironov, D., Weisensee, U., & Zittel, P. (2006). Area-averaged surface fluxes over the Litfass region based on eddy-covariance measurements. *Boundary-Layer Meteorology*, *121*(1), 33–65.

Bianco, L., Wilczak, J. M., & White, A. B. (2008). Convective boundary layer depth estimation from wind profilers: statistical comparison between an automated algorithm and expert estimations. *Journal of Atmospheric and Oceanic Technology*, *25*(8), 1397–1413.

Brady, J. M., Stokes, M. D., Bonnardel, J., & Bertram, T. H. (2016). Characterization of a quadrotor unmanned aircraft system for aerosol-particle-concentration measurements. *Environmental Science & Technology*, *50*(3), 1376–1383.

Brakke, T. W., Verma, S. B., & Rosenberg, N. J. (1978). Local and regional components of sensible heat advection. *Journal of Applied Meteorology (1962-1982)*, *17*(7), 955–963.

Brugger, P., Banerjee, T., De Roo, F., Kröniger, K., Qubaja, R., Rohatyn, S., Rotenberg, E., Tatarinov, F., Yakir, D., Yang, F., & Mauder, M. (2018). Effect of surface heterogeneity on the boundary-layer height: a case study at a semi-arid forest. *Boundary-Layer Meteorology*, *169*(2), 233–250.

Brutsaert, W. (1982). Evaporation into the Atmosphere: Theory, History, and Applications. Springer, Dordrecht, 299.

Choularton, T. W., Gallagher, M. W., Bower, K. N., Fowler, D., Zahniser, M. S., Kaye, A., Monteith, J. L., Harding, R. J., Fowler, D., Jenkinson, D. S., Monteith, J. L., & Unsworth, M. H. (1995). Trace gas flux measurements at the landscape scale using boundary-layer budgets. *Philosophical Transactions of the Royal Society of London. Series A: Physical and Engineering Sciences*, *351*(1696), 357–369.

Cleugh, H. A., & Grimmond, C. S. B. (2001). Modelling regional scale surface energy exchanges and CBL growth in a heterogeneous, urban-rural landscape. *Boundary-Layer Meteorology*, *98*(1), 1–31.

Combe, M., Vilà-Guerau de Arellano, J., Ouwersloot, H. G., & Peters, W. (2016). Plant

water-stress parameterization determines the strength of land–atmosphere coupling. *Agricultural and Forest Meteorology*, *217*, 61–73.

Compton, J. C., Delgado, R., Berkoff, T. A., & Hoff, R. M. (2013). Determination of planetary boundary layer height on short spatial and temporal scales: a demonstration of the covariance wavelet transform in ground-based wind profiler and lidar measurements. *Journal of Atmospheric and Oceanic Technology*, *30*(7), 1566–1575.

Davy, R., & Esau, I. (2016). Differences in the efficacy of climate forcings explained by variations in atmospheric boundary layer depth. *Nature Communications*, *7*(1), 11690.

Denmead, O. T., Raupach, M. R., Dunin, F. X., Cleugh, H. A., & Leuning, R. (1996). Boundary layer budgets for regional estimates of scalar fluxes. *Global Change Biology*, *2*(3), 255–264.

Denning, A. S., Fung, I. Y., & Randall, D. (1995). Latitudinal gradient of atmospheric CO_2 due to seasonal exchange with land biota. *Nature*, *376*(6537), 240–243.

Denning, A. S., Takahashi, T., & Friedlingstein, P. (1999). Can a strong atmospheric CO_2 rectifier effect be reconciled with a "reasonable" carbon budget? *Tellus B: Chemical and Physical Meteorology*, *51*(2), 249–253.

Desai, A. R., Helliker, B. R., Moorcroft, P. R., Andrews, A. E., & Berry, J. A. (2010). Climatic controls of interannual variability in regional carbon fluxes from top-down and bottom-up perspectives. *Journal of Geophysical Research: Biogeosciences*, *115,* G02011.

Driedonks, A. G. M., & Tennekes, H. (1984). Entrainment effects in the well-mixed atmospheric boundary layer. *Boundary-Layer Meteorology, 30*(1), 75–105.

Durre, I., Vose, R. S., & Wuertz, D. B. (2006). Overview of the integrated global radiosonde archive. *Journal of Climate*, *19*(1), 53–68.

Eder, F., De Roo, F., Rotenberg, E., Yakir, D., Schmid, H. P., & Mauder, M. (2015). Secondary circulations at a solitary forest surrounded by semi-arid shrubland and their impact on eddy-covariance measurements. *Agricultural and Forest Meteorology*, *211–212*, 115–127.

Eder, F., Schmidt, M., Damian, T., Träumner, K., & Mauder, M. (2015). Mesoscale eddies affect near-surface turbulent exchange: evidence from lidar and tower measurements. *Journal of Applied Meteorology and Climatology*, *54*(1), 189–206.

Ek, M. B., & Holtslag, A. A. M. (2004). Influence of Soil Moisture on Boundary Layer Cloud Development. *Journal of Hydrometeorology*, *5*(1), 86–99.

Emeis, S., Münkel, C., Vogt, S., Müller, W. J., & Schäfer, K. (2004). Atmospheric boundary-layer structure from simultaneous SODAR, RASS, and ceilometer measurements. *Atmospheric Environment*, *38*(2), 273–286.

Findell, K. L., & Eltahir, E. A. B. (2003a). Atmospheric controls on soil moisture–boundary layer interactions. Part I: Framework Development. *Journal of Hydrometeorology*, *4*(3), 552–569.

Findell, K. L., & Eltahir, E. A. B. (2003b). Atmospheric controls on soil moisture–boundary layer interactions. Part II: Feedbacks within the continental United States. *Journal of Hydrometeorology*, *4*(3), 570–583.

Ford, T. W., Quiring, S. M., Frauenfeld, O. W., & Rapp, A. D. (2015). Synoptic conditions related to soil moisture-atmosphere interactions and unorganized convection in Oklahoma. *Journal of Geophysical Research: Atmospheres*, *120*(22), 11,519-11,535.

Gentine, P., Chhang, A., Rigden, A., & Salvucci, G. (2016). Evaporation estimates using weather station data and boundary layer theory. *Geophysical Research Letters*, *43*(22), 11,661-11,670.

Gentine, Pierre, Ferguson, C. R., & Holtslag, A. A. M. (2013). Diagnosing evaporative fraction over land from boundary-layer clouds. *Journal of Geophysical Research: Atmospheres*, *118*(15), 8185–8196.

Gentine, Pierre, Holtslag, A. A. M., D'Andrea, F., & Ek, M. (2013). Surface and atmospheric controls on the onset of moist convection over land. *Journal of Hydrometeorology*, *14*(5), 1443–1462.

Gerken, T., Bromley, G. T., & Stoy, P. C. (2018). Surface moistening trends in the northern North American Great Plains increase the likelihood of convective initiation. *Journal*

of Hydrometeorology, 19(1), 227–244.

Gerken, T., Ruddell, B. L., Yu, R., Stoy, P. C., & Drewry, D. T. (2019). Robust observations of land-to-atmosphere feedbacks using the information flows of FLUXNET. *npj Climate and Atmospheric Science*, 2(1), 37.

Grant, L. D., & van den Heever, S. C. (2016). Cold pool dissipation. *Journal of Geophysical Research: Atmospheres*, 121(3), 1138–1155.

Green, J. K., Seneviratne, S. I., Berg, A. M., Findell, K. L., Hagemann, S., Lawrence, D. M., & Gentine, P. (2019). Large influence of soil moisture on long-term terrestrial carbon uptake. *Nature*, 565(7740), 476–479.

Griebel, A., Bennett, L. T., Metzen, D., Cleverly, J., Burba, G., & Arndt, S. K. (2016). Effects of inhomogeneities within the flux footprint on the interpretation of seasonal, annual, and interannual ecosystem carbon exchange. *Agricultural and Forest Meteorology*, 221, 50–60.

Griffis, T. J., Zhang, J., Baker, J. M., Kljun, N., & Billmark, K. (2007). Determining carbon isotope signatures from micrometeorological measurements: Implications for studying biosphere–atmosphere exchange processes. *Boundary-Layer Meteorology*, 123(2), 295–316.

Grimsdell, A. W., & Angevine, W. M. (1998). Convective boundary layer height Measurement with wind profilers and comparison to cloud base. *Journal of Atmospheric and Oceanic Technology*, 15, 1331-1338.

Grund, C. J., Banta, R. M., George, J. L., Howell, J. N., Post, M. J., Richter, R. A., & Weickmann, A. M. (2001). High-Resolution Doppler Lidar for boundary layer and cloud research. *Journal of Atmospheric and Oceanic Technology*, 18(3), 376–393.

Gustafson, W. I., Vogelmann, A. M., Li, Z., Cheng, X., Dumas, K. K., Endo, S., Johnson, K. L., Krishna, B., Toto, T., & Xiao, H. (2020). The Large-Eddy Simulation (LES) Atmospheric Radiation Measurement (ARM) Symbiotic Simulation and Observation (LASSO) activity for continental shallow convection. *Bulletin of the American Meteorological Society*, 101, E462-E479.

Hartery, S., Commane, R., Lindaas, J., Sweeney, C., Henderson, J., Mountain, M., Steiner, N., McDonald, K., Dinardo, S. J., Miller, C. E., Wofsy, S. C., & Chang, R. Y.-W. (2018). Estimating regional-scale methane flux and budgets using CARVE aircraft measurements over Alaska. *Atmospheric Chemistry and Physics*, *18*(1), 185–202.

Helbig, M., Waddington, J.M., Alekseychik, P. *et al.* (2020). Increasing contribution of peatlands to boreal evapotranspiration in a warming climate. *Nature Climate Change,* https://doi.org/10.1038/s41558-020-0763-7.

Helbig, M., Wischnewski, K., Kljun, N., Chasmer, L. E., Quinton, W. L., Detto, M., & Sonnentag, O. (2016). Regional atmospheric cooling and wetting effect of permafrost thaw-induced boreal forest loss. *Global Change Biology*, *22*(12), 4048–4066.

Helliker, B. R., Berry, J. A., Betts, A. K., Bakwin, P. S., Davis, K. J., Denning, A. S., Ehleringer, J. R., Miller, J. B., Butler, M. P., & Ricciuto, D. M. (2004). Estimates of net CO_2 flux by application of equilibrium boundary layer concepts to CO_2 and water vapor measurements from a tall tower. *Journal of Geophysical Research: Atmospheres*, *109,* D20106.

Hemes, K. S., Eichelmann, E., Chamberlain, S. D., Knox, S. H., Oikawa, P. Y., Sturtevant, C., Verfaillie, J., Szutu, D., & Baldocchi, D. D. (2018). A unique combination of aerodynamic and surface properties contribute to surface cooling in restored wetlands of the Sacramento-San Joaquin Delta, California. *Journal of Geophysical Research: Biogeosciences*, *123*(7), 2072–2090.

Janssen, R. H. H., Vilà-Guerau de Arellano, J., Jimenez, J. L., Ganzeveld, L. N., Robinson, N. H., Allan, J. D., Coe, H., & Pugh, T. A. M. (2013). Influence of boundary layer dynamics and isoprene chemistry on the organic aerosol budget in a tropical forest. *Journal of Geophysical Research: Atmospheres*, *118*(16), 9351–9366.

Juang, J.-Y., Katul, G. G., Porporato, A., Stoy, P. C., Siqueira, M. S., Detto, M., Kim, H.-S., & Oren, R. (2007). Eco-hydrological controls on summertime convective rainfall triggers. *Global Change Biology*, *13*, 887-896.

Juang, J.-Y., Porporato, A., Stoy, P. C., Siqueira, M. S., Oishi, A. C., Detto, M., Kim, H.-S., &

Katul, G. G. (2007). Hydrologic and atmospheric controls on initiation of convective precipitation events. *Water Resources Research*, *43*, WR004954.

Kiese, R., Fersch, B., Baessler, C., Brosy, C., Butterbach-Bahl, K., Chwala, C., Dannenmann, M., Fu, J., Gasche, R., Grote, R., Jahn, C., Klatt, J., Kunstmann, H., Mauder, M., Rödiger, T., Smiatek, G., Soltani, M., Steinbrecher, R., Völksch, I., … Schmid, H. P. (2018). The TERENO Pre-Alpine Observatory: Integrating meteorological, hydrological, and biogeochemical measurements and modeling. *Vadose Zone Journal*, *17*(1), 180060.

Kljun, N., Calanca, P., Rotach, M. W., & Schmid, H. P. (2015). A simple two-dimensional parameterisation for Flux Footprint Prediction (FFP). *Geoscientific Model Development*, *8*(11), 3695–3713.

Knohl, A., & Baldocchi, D. D. (2008). Effects of diffuse radiation on canopy gas exchange processes in a forest ecosystem. *Journal of Geophysical Research: Biogeosciences*, *113,* G02023.

Konings, A. G., Katul, G. G., & Porporato, A. (2010). The rainfall-no rainfall transition in a coupled land-convective atmosphere system. *Geophysical Research Letters*, *37*, L14401.

Koster, R. D., Schubert, S. D., & Suarez, M. J. (2009). Analyzing the concurrence of meteorological droughts and warm periods, with implications for the determination of evaporative regime. *Journal of Climate*, *22*(12), 3331–3341.

Kotthaus, S., & Grimmond, C. S. B. (2018a). Atmospheric boundary-layer characteristics from ceilometer measurements. Part 1: A new method to track mixed layer height and classify clouds. *Quarterly Journal of the Royal Meteorological Society*, *144*(714), 1525–1538.

Kröniger, K., De Roo, F., Brugger, P., Huq, S., Banerjee, T., Zinsser, J., Rotenberg, E., Yakir, D., Rohatyn, S., & Mauder, M. (2018). Effect of secondary circulations on the surface–atmosphere exchange of energy at an isolated semi-arid forest. *Boundary-Layer Meteorology*, *169*(2), 209–232.

Kotthaus, S., & Grimmond, C. S. B. (2018b). Atmospheric boundary-layer characteristics from ceilometer measurements. Part 2: Application to London's urban boundary layer. *Quarterly Journal of the Royal Meteorological Society*, *144*(714), 1511–1524.

Lang, A. R. G., Evans, G. N., & Ho, P. Y. (1974). The influence of local advection on evapotranspiration from irrigated rice in a semi-arid region. *Agricultural Meteorology*, *13*(1), 5–13.

Lang, A. R. G., McNaughton, K. G., Fazu, C., Bradley, E. F., & Ohtaki, E. (1983). An experimental appraisal of the terms in the heat and moisture flux equations for local advection. *Boundary-Layer Meteorology*, *25*(1), 89–102.

Lansu, E. M., Heerwaarden, C. C. van, Stegehuis, A. I., & Teuling, A. J. (2020). Atmospheric aridity and apparent soil moisture drought in European forest during heat waves. *Geophysical Research Letters*, *47*(6), e2020GL087091.

Lauvaux, T., & Davis, K. J. (2014). Planetary boundary layer errors in mesoscale inversions of column-integrated CO_2 measurements. *Journal of Geophysical Research: Atmospheres*, *119*(2), 490–508.

Lin, J. C., Gerbig, C., Wofsy, S. C., Andrews, A. E., Daube, B. C., Davis, K. J., & Grainger, C. A. (2003). A near-field tool for simulating the upstream influence of atmospheric observations: The Stochastic Time-Inverted Lagrangian Transport (STILT) model. *Journal of Geophysical Research: Atmospheres*, *108,* 4493.

Luyssaert, S., Jammet, M., Stoy, P. C., Estel, S., Pongratz, J., Ceschia, E., Churkina, G., Don, A., Erb, K., Ferlicoq, M., Gielen, B., Grünwald, T., Houghton, R. A., Klumpp, K., Knohl, A., Kolb, T., Kuemmerle, T., Laurila, T., Lohila, A., Dolman, A. J. (2014). Land management and land-cover change have impacts of similar magnitude on surface temperature. *Nature Climate Change*, *4*(5), 389–393.

Manoli, G., Domec, J.-C., Novick, K., Oishi, A. C., Noormets, A., Marani, M., & Katul, G. (2016). Soil-plant-atmosphere conditions regulating convective cloud formation above southeastern US pine plantations. *Global Change Biology*, *22*(6), 2238–2254.

McColl, K. A., & Rigden, A. J. (2020). Emergent simplicity of continental evapotranspiration.

Geophysical Research Letters, *47*(6), e2020GL087101.

McGrath-Spangler, E. L., Molod, A., Ott, L. E., & Pawson, S. (2015). Impact of planetary

boundary layer turbulence on model climate and tracer transport. *Atmospheric*

Chemistry and Physics, *15*(13), 7269–7286.

McNaughton, K. G., & Spriggs, T. W. (1986). A mixed-layer model for regional evaporation.

Boundary-Layer Meteorology, *34*(3), 243–262.

Miralles, D. G., Gentine, P., Seneviratne, S. I., & Teuling, A. J. (2019). Land-atmospheric

feedbacks during droughts and heatwaves: state of the science and current

challenges: Land feedbacks during droughts and heatwaves. *Annals of the New York*

Academy of Sciences, *1436*(1), 19–35.

Miralles, D. G., Teuling, A. J., van Heerwaarden, C. C., & Vilà-Guerau de Arellano, J. (2014).

Mega-heatwave temperatures due to combined soil desiccation and atmospheric

heat accumulation. *Nature Geoscience*, *7*(5), 345–349.

Molod, A., Salmun, H., & Dempsey, M. (2015). Estimating planetary boundary layer heights

from NOAA Profiler Network Wind Profiler data. *Journal of Atmospheric and Oceanic*

Technology, *32*(9), 1545–1561.

Monin, A.S., & Obukhov, A.M. (1954). Osnovnye zakonomernosti turbulentnogo

peremeshivanija v prizemnom sloe atmosfery (Basic Laws of Turbulent Mixing in the

Atmosphere Near the Ground). Trudy geofiz. inst. AN SSSR 24(151): 163–187.

Neggers, R. A. J., Siebesma, A. P., & Heus, T. (2012). Continuous single-column model

evaluation at a permanent meteorological supersite. *Bulletin of the American*

Meteorological Society, *93*(9), 1389–1400.

Novick, K. A., & Katul, G. G. (2020). The duality of reforestation impacts on surface and air

temperature. *Journal of Geophysical Research: Biogeosciences*, *125*(4),

e2019JG005543.

Panwar, A., Kleidon, A., & Renner, M. (2019). Do surface and air temperatures contain

similar imprints of evaporative conditions? *Geophysical Research Letters*, *46*(7),

3802–3809.

Patton, E. G., Sullivan, P. P., Shaw, R. H., Finnigan, J. J., & Weil, J. C. (2016). Atmospheric stability influences on coupled boundary layer and canopy turbulence. *Journal of the Atmospheric Sciences*, *73*(4), 1621–1647.

Pedruzo-Bagazgoitia, X., Ouwersloot, H. G., Sikma, M., van Heerwaarden, C. C., Jacobs, C. M. J., & Vilà-Guerau de Arellano, J. (2017). Direct and diffuse radiation in the shallow cumulus–vegetation system: enhanced and decreased evapotranspiration regimes. *Journal of Hydrometeorology*, *18*(6), 1731–1748.

Prabha, T. V., Leclerc, M. Y., Karipot, A., Hollinger, D. Y., & Mursch-Radlgruber, E. (2008). Influence of nocturnal low-level jets on eddy-covariance fluxes over a tall forest canopy. *Boundary-Layer Meteorology*, *126*(2), 219–236.

Priestley, C. H. B., & Taylor, R. J. (1972). On the assessment of surface heat flux and evaporation using large-scale parameters. *Monthly Weather Review*, *100*(2), 81–92.

Raupach, M. R. (1998). Influences of local feedbacks on land–air exchanges of energy and carbon. *Global Change Biology*, *4*(5), 477–494.

Raupach, M. R. (2000). Equilibrium evaporation and the convective boundary layer. *Boundary-Layer Meteorology*, *96*(1), 107–142.

Raupach, M. R. (2001). Combination theory and equilibrium evaporation. *Quarterly Journal of the Royal Meteorological Society*, *127*(574), 1149–1181.

Raupach, M.R., & Thom, A.S. (1981). Turbulence in and above plant canopies. *Annual Review of Fluid Mechanics*, *13(1)*, 97-129.

Raupach, M. R., Denmead, O. T., & Dunin, F. X. (1992). Challenges in linking atmospheric CO_2 concentrations to fluxes at local and regional scales. *Australian Journal of Botany*, *40*(5), 697–716.

Rigden, A. J., & Salvucci, G. D. (2015). Evapotranspiration based on equilibrated relative humidity (ETRHEQ): Evaluation over the continental U.S. *Water Resources Research*, *51*(4), 2951–2973.

De Roo, F. D., Zhang, S., Huq, S., & Mauder, M. (2018). A semi-empirical model of the energy balance closure in the surface layer. *PLOS ONE*, *13*(12), e0209022.

Salcido, A., Celada-Murillo, A.-T., Carreón-Sierra, S., Castro, T., Peralta, O., Salcido-González, R.-S., Hernández-Flores, N., Tamayo-Flores, G.-A., & Martínez-Flores, M.-A. (2020). Estimations of the Mexicali Valley (Mexico) mixing height. *Atmosphere*, *11*(5), 505.

Salvucci, G. D., & Gentine, P. (2013). Emergent relation between surface vapor conductance and relative humidity profiles yields evaporation rates from weather data. *Proceedings of the National Academy of Sciences*, *110*(16), 6287–6291.

Sanchez-Mejia, Z. M., & Papuga, S. A. (2014). Observations of a two-layer soil moisture influence on surface energy dynamics and planetary boundary layer characteristics in a semiarid shrubland. *Water Resources Research*, *50*, 306–317.

Sanchez-Mejia, Z. M., & Papuga, S. A. (2017). Empirical modeling of planetary boundary layer dynamics under multiple precipitation scenarios using a two-layer soil moisture approach: An Example From a Semiarid Shrubland. *Water Resources Research*, *53*, 8807–8824.

Santanello, J. A., Dirmeyer, P. A., Ferguson, C. R., Findell, K. L., Tawfik, A. B., Berg, A., Ek, M., Gentine, P., Guillod, B. P., van Heerwaarden, C., Roundy, J., & Wulfmeyer, V. (2017). Land–atmosphere interactions: the LoCo perspective. *Bulletin of the American Meteorological Society*, *99*(6), 1253–1272.

Santanello, J. A., Peters-Lidard, C. D., & Kumar, S. V. (2011). Diagnosing the sensitivity of local land–atmosphere coupling via the soil moisture–boundary layer interaction. *Journal of Hydrometeorology*, *12*(5), 766–786.

Seibert, P., Beyrich, F., Gryning, S.-E., Joffre, S., Rasmussen, A., & Tercier, P. (2000). Review and intercomparison of operational methods for the determination of the mixing height. *Atmospheric Environment*, *34*(7), 1001–1027.

Seneviratne, S. I., Corti, T., Davin, E. L., Hirschi, M., Jaeger, E. B., Lehner, I., Orlowsky, B., & Teuling, A. J. (2010). Investigating soil moisture–climate interactions in a changing climate: A review. *Earth-Science Reviews*, *99*(3–4), 125–161.

Shen, S. & Leclerc, M.Y. (1995). How large must surface inhomogeneities be before they

influence the convective boundary layer structure? A case study. Q.J.R. Meteorol. Soc., *121*, 1209-1228.

Shuttleworth, W. J., Serrat-Capdevila, A., Roderick, M. L., & Scott, R. L. (2009). On the theory relating changes in area-average and pan evaporation. *Quarterly Journal of the Royal Meteorological Society*, *135*(642), 1230-1247.

Sikma, M., & Vilà-Guerau de Arellano, J. (2019). Substantial reductions in cloud cover and moisture transport by dynamic plant responses. *Geophysical Research Letters*, *46*(3), 1870–1878.

Siqueira, M., Katul, G., & Porporato, A. (2009). Soil moisture feedbacks on convection triggers: the role of soil–plant hydrodynamics. *Journal of Hydrometeorology*, *10*(1), 96–112.

Stein, A. F., Draxler, R. R., Rolph, G. D., Stunder, B. J. B., Cohen, M. D., & Ngan, F. (2015). NOAA's HYSPLIT Atmospheric Transport and Dispersion Modeling System. *Bulletin of the American Meteorological Society*, *96*(12), 2059–2077.

Stoy, P. C., Mauder, M., Foken, T., Marcolla, B., Boegh, E., Ibrom, A., Arain, M. A., Arneth, A., Aurela, M., Bernhofer, C., Cescatti, A., Dellwik, E., Duce, P., Gianelle, D., van Gorsel, E., Kiely, G., Knohl, A., Margolis, H., McCaughey, H., … Varlagin, A. (2013). A data-driven analysis of energy balance closure across FLUXNET research sites: The role of landscape scale heterogeneity. *Agricultural and Forest Meteorology*, *171–172*, 137–152.

Stull, R. B. (1988). Mean boundary layer characteristics. In R. B. Stull (Ed.), *An Introduction to Boundary Layer Meteorology* (pp. 1–27). Springer Netherlands.

Thomas, C., & Foken, T. (2007). Flux contribution of coherent structures and its implications for the exchange of energy and matter in a tall spruce canopy. *Boundary-Layer Meteorology*, *123*(2), 317–337.

Tucker, S. C., Senff, C. J., Weickmann, A. M., Brewer, W. A., Banta, R. M., Sandberg, S. P., Law, D. C., & Hardesty, R. M. (2009). Doppler lidar estimation of mixing height using turbulence, shear, and aerosol profiles. *Journal of Atmospheric and Oceanic*

Technology, *26*(4), 673–688.

van Heerwaarden, C. C., Vilà-Guerau de Arellano, J., Moene, A. F., & Holtslag, A. A. M. (2009). Interactions between dry-air entrainment, surface evaporation and convective boundary-layer development. *Quarterly Journal of the Royal Meteorological Society*, *135*(642), 1277–1291.

van Stratum, B. J. H., Vilá-Guerau de Arellano, J., van Heerwaarden, C. C., & Ouwersloot, H. G. (2014). Subcloud-layer feedbacks driven by the mass flux of shallow cumulus convection over land. *Journal of the Atmospheric Sciences*, *71*(3), 881–895.

Venkatram, A. (1977). A model of internal boundary-layer development. *Boundary-Layer Meteorology*, *11*(4), 419–437.

Vesala, T., Kljun, N., Rannik, Ü., Rinne, J., Sogachev, A., Markkanen, T., Sabelfeld, K., Foken, Th., & Leclerc, M. Y. (2008). Flux and concentration footprint modelling: State of the art. *Environmental Pollution*, *152*(3), 653–666.

Vick, E. S. K., Stoy, P. C., Tang, A. C. I., & Gerken, T. (2016). The surface-atmosphere exchange of carbon dioxide, water, and sensible heat across a dryland wheat-fallow rotation. *Agriculture, Ecosystems & Environment*, *232*, 129–140.

Vila-Guerau de Arellano, J., C. van Heerwaarden, C., J. H. van Stratum, B., & van den Dries, K. (2015). *Atmospheric Boundary Layer: Integrating Air Chemistry and Land Interactions*. Cambridge University Press.

Vilà-Guerau de Arellano, J., Ouwersloot, H. G., Baldocchi, D., & Jacobs, C. M. J. (2014). Shallow cumulus rooted in photosynthesis. *Geophysical Research Letters*, *41*(5), 1796–1802.

Vilà-Guerau de Arellano, J., Patton, E. G., Karl, T., van den Dries, K., Barth, M. C., & Orlando, J. J. (2011). The role of boundary layer dynamics on the diurnal evolution of isoprene and the hydroxyl radical over tropical forests. *Journal of Geophysical Research: Atmospheres*, *116,* D07304.

Vilà-Guerau de Arellano, J., van Heerwaarden, C. C., & Lelieveld, J. (2012). Modelled suppression of boundary-layer clouds by plants in a CO2-rich atmosphere. *Nature*

Geoscience, 5(10), 701–704.

Vogel, M. M., Orth, R., Cheruy, F., Hagemann, S., Lorenz, R., Hurk, B. J. J. M., & Seneviratne, S. I. (2017). Regional amplification of projected changes in extreme temperatures strongly controlled by soil moisture-temperature feedbacks. *Geophysical Research Letters, 44*(3), 1511–1519.

Wang, W., Davis, K. J., Cook, B. D., Yi, C., Butler, M. P., Ricciuto, D. M., & Bakwin, P. S. (2007). Estimating daytime CO_2 fluxes over a mixed forest from tall tower mixing ratio measurements. *Journal of Geophysical Research: Atmospheres, 112,* D10308.

Wang, W., Davis, K. J., Ricciuto, D. M., & Butler, M. P. (2006). An approximate footprint model for flux measurements in the convective boundary layer. *Journal of Atmospheric and Oceanic Technology, 23*(10), 1384–1394.

Wang, X. Y., & Wang, K. C. (2014). Estimation of atmospheric mixing layer height from radiosonde data. *Atmospheric Measurement Techniques, 7*(6), 1701–1709.

Wesely, M. L. (1976). The combined effect of temperature and humidity fluctuations on refractive index. *Journal of Applied Meteorology, 15*(1), 43–49.

Wharton, S., Ma, S., Baldocchi, D. D., Falk, M., Newman, J. F., Osuna, J. L., & Bible, K. (2017). Influence of regional nighttime atmospheric regimes on canopy turbulence and gradients at a closed and open forest in mountain-valley terrain. *Agricultural and Forest Meteorology, 237–238*, 18–29.

White, A. B., Fairall, C. W., & Thomson, D. W. (1991). Radar observations of humidity variability in and above the marine atmospheric boundary layer. *Journal of Atmospheric and Oceanic Technology, 8*(5), 639–658.

Wilczak, J. M., Gossard, E. E., Neff, W. D., & Eberhard, W. L. (1996). Ground-based remote sensing of the atmospheric boundary layer: 25 years of progress. *Boundary-Layer Meteorology, 78*(3), 321–349.

Wofsy, S. C., Harriss, R. C., & Kaplan, W. A. (1988). Carbon dioxide in the atmosphere over the Amazon Basin. *Journal of Geophysical Research: Atmospheres, 93*(D2), 1377–1387.

Wolf, S., Keenan, T. F., Fisher, J. B., Baldocchi, D. D., Desai, A. R., Richardson, A. D., Scott, R. L., Law, B. E., Litvak, M. E., Brunsell, N. A., Peters, W., & van der Laan-Luijkx, I. T. (2016). Warm spring reduced carbon cycle impact of the 2012 US summer drought. *Proceedings of the National Academy of Sciences*, *113*(21), 5880–5885.

Wood, C. R., Järvi, L., Kouznetsov, R. D., Nordbo, A., Joffre, S., Drebs, A., Vihma, T., Hirsikko, A., Suomi, I., Fortelius, C., O'Connor, E., Moiseev, D., Haapanala, S., Moilanen, J., Kangas, M., Karppinen, A., Vesala, T., & Kukkonen, J. (2013). An overview of the urban boundary layer atmosphere network in Helsinki. *Bulletin of the American Meteorological Society*, *94*(11), 1675–1690.

Wouters, H., Petrova, I. Y., van Heerwaarden, C. C., Vilà-Guerau de Arellano, J., Teuling, A. J., Meulenberg, V., Santanello, J. A., & Miralles, D. G. (2019). Atmospheric boundary layer dynamics from balloon soundings worldwide: CLASS4GL v1.0. *Geoscientific Model Development*, *12*, 2139-2153.

Wyngaard, J. C., & Brost, R. A. (1984). Top-down and bottom-up diffusion of a scalar in the convective boundary layer. *Journal of the Atmospheric Sciences*, *41*(1), 102–112.

Xu, K., Metzger, S., & Desai, A. R. (2017). Upscaling tower-observed turbulent exchange at fine spatio-temporal resolution using environmental response functions. *Agricultural and Forest Meteorology*, *232*, 10–22.

Xu, K., Sühring, M., Metzger, S., Durden, D., & Desai, A. R. (2020). Can data mining help eddy covariance see the landscape? A large-eddy simulation study. *Boundary-Layer Meteorology*. https://doi.org/10.1007/s10546-020-00513-0

Yi, C., Davis, K. J., Bakwin, P. S., Berger, B. W., & Marr, L. C. (2000). Influence of advection on measurements of the net ecosystem-atmosphere exchange of CO_2 from a very tall tower. *Journal of Geophysical Research: Atmospheres*, *105*(D8), 9991–9999. https://doi.org/10.1029/2000JD900080

Yi, C., Davis, K. J., Bakwin, P. S., Denning, A. S., Zhang, N., Desai, A., Lin, J. C., & Gerbig, C. (2004). Observed covariance between ecosystem carbon exchange and

atmospheric boundary layer dynamics at a site in northern Wisconsin. *Journal of Geophysical Research: Atmospheres*, *109*(D8), 9991-9999.

Yi, C., Davis, K. J., Berger, B. W., & Bakwin, P. S. (2001). Long-term observations of the dynamics of the continental planetary boundary layer. *58*, 1288-1299.

Yin, J., Gao, C. Y., Hong, J., Gao, Z., Li, Y., Li, X., Fan, S., & Zhu, B. (2019). Surface meteorological conditions and boundary layer height variations during an air Pollution episode in Nanjing, China. *Journal of Geophysical Research: Atmospheres*, *124*(6), 3350–3364.

Yin, J., Albertson, J. D., Rigby, J. R., & Porporato, A. (2015). Land and atmospheric controls on initiation and intensity of moist convection: CAPE dynamics and LCL crossings. *Water Resources Research*, *51*(10), 8476–8493.

Zhao, C., Andrews, A. E., Bianco, L., Eluszkiewicz, J., Hirsch, A., MacDonald, C., Nehrkorn, T., & Fischer, M. L. (2009). Atmospheric inverse estimates of methane emissions from Central California. *Journal of Geophysical Research: Atmospheres*, *114,* D16302.

Zilitinkevich, S. S., Tyuryakov, S. A., Troitskaya, Yu. I., & Mareev, E. A. (2012). Theoretical models of the height of the atmospheric boundary layer and turbulent entrainment at its upper boundary. *Izvestiya, Atmospheric and Oceanic Physics*, *48*(1), 133–142.

List of breakout session attendees at the AmeriFlux Annual Meeting 2019 ("Extending atmospheric boundary layer observations across the AmeriFlux network")

Breakout session lead: Manuel Helbig, *McMaster University*

Scott Bender, *Physical Sciences Inc.*

Sebastien Biraud, *Lawrence Berkeley National Laboratory*

Nathaniel Brunsell, *University of Kansas*

Sean Burns, *University of Colorado & National Center for Atmospheric Research*

Stephen Chan, *Lawrence Berkeley National Laboratory*

Tomer Duman, *University of New Mexico*

Chad Hanson, *Oregon State University*

Giacomo Nicolini, *University of Tuscia*

Kimberley Novick, *Indiana University-Bloomington*

Steve Oncley, *National Center for Atmospheric Research*

Prajaya Prajapati, *Texas A&M University*

Andrew Richardson, *Northern Arizona University*

Bijan Seyednasrollah, *Northern Arizona University*

Gabriela Shirkey, *Michigan State University*

David Sonnenfroh, *Physical Sciences Inc.*

Ryan Sullivan, *Argonne National Laboratory*

Paul Stoy, *University of Wisconsin-Indiana*